JPL PUBLICATION 80-11

Beamed Microwave Power Transmitting and Receiving Subsystems Radiation Characteristics

Richard M. Dickinson

June 15, 1980

National Aeronautics and
Space Administration

Jet Propulsion Laboratory
California Institute of Technology
Pasadena, California

JPL PUBLICATION 80-11

Beamed Microwave Power Transmitting and Receiving Subsystems Radiation Characteristics

Richard M. Dickinson

June 15, 1980

National Aeronautics and
Space Administration

Jet Propulsion Laboratory
California Institute of Technology
Pasadena, California

FOREWORD AND ACKNOWLEDGMENTS

This report is one facet of NASA's investigation of the technology associated with the concept of Beamed Microwave Power, performed by the Telecommunications Science and Engineering Division of the Jet Propulsion Laboratory.

Particular thanks are extended to the personnel of the Radio Frequency and Microwave Section and the Spacecraft Telecommunications Equipment Section, for their assistance and participation in the designing, fabricating, and checkout of the equipment, and in the recording of the experimental measurements.

This investigation was performed under the program guidance of Mr. Simon V. Manson of the Space Utilization Systems, Energy Systems Division of the Office of Aeronautics and Space Technology, NASA Headquarters.

The author acknowledges the following people for their review of the first draft of this report:

W. C. Brown
Raytheon Co.
Microwave & Power Tube Div.
Foundary Ave.
Waltham MA 02154

W. Finnell III
Code PD-14
NASA Marshall Spaceflight Ctr.
Huntsville AL 35812

R. J. Gutman
Associate Professor
Electrical & Systems
Engineering Dept.
Rensselaer Polytechnic
Institute
Troy NY 12181

S. V. Manson
Code RES-1
NASA Headquarters
Washington DC 20546

R. P. Mathison
Manager, Telecommunications
Science & Engineering Div.
Jet Propulsion Laboratory
4800 Oak Grove Dr.
Pasadena CA 91103

E. J. Nalos
Boeing Aerospace Corp.
Seattle WA 92124

W. V. T. Rusch
Professor of Electrical
Engineering
School of Engineering
University of Southern
California
Los Angeles CA 90007

EXECUTIVE SUMMARY

This paper reports the results of an experimental project for determining the approximate levels and spatial distribution patterns of noise, harmonic and fundamental frequency radiations from components similar to those proposed for Beamed Power Systems. The measured results may be extrapolated and used in connection with projected applicable radio regulations to determine the required RF filtering that will permit legitimate operation in beamed power service.

Laboratory tests and other controlled demonstrations of microwave transmitting and receiving systems have achieved impressive power-density handling performance and operating efficiencies. The basic technology is adequate for proposed applications of beamed power such as supplying aerostat station-keeping, propulsion or payload power, aircraft flight power, or the currently envisioned Satellite Power Systems (SPS). However, today's small-scale achievements were gained without the encumbrances that may be necessary for meeting tomorrow's applicable electromagnetic compatibility and safety requirements for the full-scale systems.

Because of a lack of good analytic models, measured characteristics of wireless power transmission system elements are necessary to provide reasonable data from which system designers and analysts might better determine the radiated signal frequency spectrum, levels, and direction. These determinations are used to scope the RF filtering task, and assess its impact on performance.

For the transmitter end of the wireless power transmitting links, previously measured spectrum data were reviewed, and additional measurements were made to characterize the dc-to-RF power converters employed to generate the high-power microwaves. Reported data on noise around the carrier, measurements of harmonic levels, and other parameters were collected for available S-band (2.1 to 2.45 GHz) klystrons, magnetrons, and solid-state power amplifiers. In general, the tube-type dc-to-RF converters' spectral noise power density in a 4 kHz bandwidth is on the order of 120 dB below the fundamental 2.45 GHz carrier at the Industrial, Scientific and Medical (ISM) band edge, 50 MHz away from the carrier. The measured harmonics for all converters depend upon the tuning, drive level, degree of saturation, temperature, and other parameters. The solid-state devices had the highest level of second harmonic output relative to the fundamental. The second harmonics for all measured data collected range from 32 to 50 dB below the carrier (dBc). The third and fourth harmonics were between 38 and 70 dBc. The fifth harmonics levels ranged from 58 to 70 dBc.

The relative magnitudes and angular radiation distribution patterns of harmonics from both an 8-slot stick and an 8-stick by 8-slot (64-element) subarray of slotted waveguides were measured to obtain data on the characteristics of RF power-radiating antennas which would likely handle the converter output RF signals. Because of the multimode propagation characteristics (permitting RF energy transport by a plurality of simultaneous but independent electric and magnetic field distributions that vary in orientation and spatially within the transmission

cavity) of the harmonics in the waveguide, the measured patterns are a function of the guide feeding arrangement and the routing details of power transport within the guide. Due to the very complex radiation patterns resulting from the multimode harmonic excitation (essentially, a very random collection of grating lobes due to the significant variation in the amplitude and phases of the harmonics in the slots of the aperture), the "average" character of the results are described by "envelope" patterns of which the $\cos^n$ family is employed. On average, the single-stick harmonic patterns could be bounded by a $\cos^3$ envelope whose peak level was 18 dB below the fundamental frequency absolute gain of +15.3 dB relative to isotropic (dBi). (An isotropic antenna has a gain of 0 dBi or unity, since by definition it radiates uniformly in all directions.) Due to a larger collection of phase and amplitude errors, the envelope bounding the harmonics from the 64-element slotted waveguide subarray was much broader in angle, and best fit a $\cos^{1.4}$ pattern shape. Also, the peak of the harmonics envelope was -52 dB relative to the +25.42 dBi gain fundamental pattern peak. The odd harmonics were generally of higher gain than the even harmonics over most of the measured hemisphere in front of the slots. Patterns to the fifth harmonic were measured and recorded.

To collect measured data relative to the receiving end of the beamed power transmission link, the rescattered fundamental and harmonic emissions to the fourth harmonic were recorded for a 6 by 7 (42-element) subarray receiving antenna (rectenna) for various load and illumination conditions. The fundamental radiation that was rescattered by the rectenna can be fit by a $\cos^{1.8}$ pattern shape over the front 60 degrees, for illumination of sufficient intensity to turn on the diodes. Under conditions of very low-level intensity illumination, the resulting rectenna impedance mismatch leads to a strongly correlated reflection as from a high-gain antenna or mirror instead of the normal diffuse or wide-angle scatter pattern. The second harmonic has a null on axis, as would be expected from the balanced dipole form of rectenna, but the peaks of radiation off boresight are only about 20 dB down from the peak incident flux density. The fourth harmonic level is higher than the third.

The rectenna -3 dB output dc power bandwidth was $\pm$15%. Depending upon the tuning pattern of the input transformer matching screws, the tuned input waveguide 1.5:1 voltage standing-wave ratio (VSWR) bandwidth for the resonant broadwall-slotted waveguide subarray ranged from a maximum of $\pm$2% to a minimum of $\pm$0.4%.

The reported measurement results provide initial reference points for Beamed-Power-System analysts and designers to engineer and assess the performance of wireless microwave power applications. The data also provide a point of departure for development of mitigation strategies for filtering the undesired, radiated noise and harmonics from beamed microwave power systems. For example, the narrow bandwidth of the resonant slotted waveguide subarray antenna may be of considerable advantage in suppressing undesired radiation at frequencies outside the ISM band. Nevertheless, considerable additional filtering of harmonics will probably be required, in particular for the SPS application of beamed power, wherein the transmitting array must handle on the order

of 5 GW and the array is visible from an entire hemisphere. The added insertion loss will affect the power transfer efficiency, increase system weight and cost, and decrease the multipacting RF power breakdown margin.

It is concluded from analyzing the measurements and from understanding the uncertainties in extrapolating the data to very large systems, that the design and construction of a modest-power-level application of beamed RF power would be technically feasible. A beamed-power aerostat or aircraft experiment could be of interest. The resulting detailed design, environmental impact statement, construction and operating permits, frequency authorizations, and performance monitoring would go a long way toward defining requirements that are likely to be imposed by society and the marketplace on a full-scale beamed power microwave transmitting and receiving system.

ABSTRACT

Measured characteristics of the spectrum of typical converters and the distribution of radiated Radio Frequency (RF) energy from the terminals (transmitting antenna and rectenna) of a beamed microwave power subsystem are presented for small transmitting and receiving S-band (2.45 GHz) subarrays.

Noise and harmonic levels of tube and solid-state RF power amplifiers are shown. RF patterns and envelopes of a 64-element slotted waveguide antenna are given for the fundamental frequency and harmonics through the fifth. Reflected fundamental and harmonic patterns through the fourth for a 42-element rectenna subarray are presented for various dc load and illumination conditions. Bandwidth measurements for the waveguide antenna and rectenna are shown.

CONTENTS

Figures

Figures

Tables

SECTION I

INTRODUCTION

Beamed RF power transmission system elements have individually demonstrated efficiencies that are satisfactory for projected beam power requirements (References 1-1, 1-2, 1-3, 1-4). Nevertheless, there remains much detailed design, development, and verification testing to be performed on the total collection of required interconnecting elements such as filters for suppression of noise and harmonic emissions and harmonic regeneration. Such filters may be necessary for simultaneously meeting applicable regulatory requirements and attaining a low insertion-transmission loss magnitude. A byproduct of the beaming of power is the undesired generation and radiation of RF harmonics and noise both at the transmitting antenna (trantenna) and receiving antenna (rectenna) terminals of the power transfer link. Also, the misfocused or spillover and rescattered fundamental frequency RF energy can be lumped in the same undesired category.

The overall engineering design of a microwave power transmitting system is primarily concerned with maximizing the efficient transmission of energy once converted to RF. Additionally, the system designers must simultaneously produce a design such that the level and direction of the undesired radiations are acceptable in terms of applicable national and international radio regulations (Reference 1-5). Systems trade-offs exist between RF filter insertion loss and RF breakdown margin at the fundamental frequency, and the cost and weight of producing the required insertion-loss or reflection at the undesired signal frequencies. Absorption-type filter design must also contend with the attendant waste heat dissipation requirements. Also, an assessment must be made of the cost of scheduled and unscheduled maintenance of both the trantenna and rectenna for continued acceptable system performance.

Propagation conditions and their effect on both the pilot beam and the power beam represent a very difficult design element to accommodate in beamed-power links. This is because the control of the propagation conditions is not under the direct influence of the system designer. Multipath propagation, absorption, scattering, refraction, and dispersion are effects that must be modeled, analyzed, and accommodated in the system design. Certain proposed applications in particular configurations or surroundings may not be able to meet applicable radio regulations when attempted at certain power levels and RF frequency bands. Altitudes and locations or orientations relative to the Earth's magnetic field may also be factors that have a bearing on the power-beam link design acceptability.

Severe weather effects such as scatter from hail may require occasional temporary cessation or curtailment of power-beaming activities, or else tolerance by those users of the radio spectrum affected by the scattered energy. Obstruction of the beam by other objects such as birds, bats, grasshoppers, aircraft, or spacecraft may also necessitate a temporary change in operations in order to stay within the permitted radio regulations or safety requirements.

This report deals principally with the performance of the microwave equipment. The characterization of the propagation medium and its effect on a high-intensity microwave Beamed Power System (and vice versa) will be discussed briefly for completeness, but will not be treated in detail herein. The equipment radiating-reception characteristics dealt with in this report are needed for such an effects study, however.

To provide technical data (additional to that available in the Bibliography) to assist the system designers and analysts, an experimental measurement program was undertaken that collected noise and harmonic data on klystrons, magnetrons, and silicon bipolar, solid-state RF power amplifiers at S-band frequencies. Such measurements are required because only a limited amount of reliable data is available on the true harmonic levels of various high-power amplifiers. The accurate measurement is difficult to perform at best, and is costly due to the peculiar requirements for extensive microwave frequency instrumentation (signal generators, calibrated insertion loss devices, filters, etc.) capable of high-power operation at all the various harmonics. Consequently, such measurements are rarely performed. Most ordinary laboratory microwave instruments are incapable of surviving the high RF power levels, and the normal alternate technique of sampling a reduced portion of the power amplifier output with a coupling device is fraught with ambiguities and inaccuracies due to the multimode nature of harmonic propagation (Reference 1-6). In a waveguide or coax transmission line large enough to safely carry the large amplitude levels of fundamental energy, the simple directional coupler RF probing scheme tends not to include a portion of all the harmonic energy propagating.

The high power output level at the fundamental carrier frequency also makes the measurement of the noise levels around the carrier expensive due to the necessity for complex instrumentation to separate the carrier and the low-level noise signals.

Adequate theory (Reference 1-7) to permit accurate analytical prediction of the expected level of noise and harmonics of the various power amplifiers is unavailable at present. Only recently have extensive computer programs (Reference 1-8) become available for modeling the exceedingly nonlinear processes inside high-power amplifiers. Moreover, because of generally unknown impedance and coupling parameters at higher frequencies, the programs are limited to modeling the fundamental carrier performance. Therefore, to provide reasonable data at this time, it is necessary to perform measurements with available equipment on existing amplifiers.

A similar problem exists with respect to the patterns of harmonics radiated from antennas. The wide-frequency-range instrumentation is complex and expensive. The multimode harmonic frequency propagation characteristics result in very complex radiating current distributions on the antenna surfaces. The current distributions and consequently the patterns change magnitude and direction as a function of the method and point of excitation in the microwave transmission line system. Again, we are short of analytic models (Reference 1-9) for arriving at the current distributions from which patterns could be calculated, and

so must resort to measurements with applicable hardware and representative descriptions of their patterns in order to describe the phenomena. Slotted waveguide antennas, which will be used in a companion project of beam-pointing verification measurements of a pilot beam-steered retrodirective array, were used to obtain harmonic radiation patterns and levels.

Finally, a small rectenna subarray was used to record rescattered fundamental (Reference 1-10) and also harmonic radiation emission patterns. Each element in the Beamed Power System and the measurement results along with any applicable theory is presented and discussed in the following sections. Also, any mitigating strategies and pertinent parameters will be discussed for potential use in future designs and applications.

SECTION II

TRANTENNA RADIATIONS

The following material will primarily deal with S-band frequencies of operation as amplified by RF power tubes, either klystrons or phase injection-locked magnetrons. The transmitting end (trantenna) of the Beamed Power System is assumed to be a phased array.

A. THE POWER BEAM SPECTRUM

The microwave power radiated from a Beamed Power System employing an active retrodirective array form of trantenna is the end product of an extremely complex chain of transfer functions. Each link of the chain, while performing its required function, makes a contribution to the resulting spectrum or modifies the spectrum of the signals input to it. It is noteworthy that the spectrum of the high-power RF signals issuing from a microwave power transmitting phased array may in part be determined by the component elements in the frequency-multiplier power supply for a pilot-tone generator, or in the high-voltage regulator circuit of the pilot-beam transmitter output amplifier located in the rectenna. Because the trantenna is a high-power device and must operate in a portion of the heavily regulated radio spectrum, its complete transmitter chain design, manufacture, assembly, and maintenance will require great attention to detail in order to adequately minimize noise and undesired signals.

The power beam output spectrum consists of the desired, nearly monochromatic carrier that is phase and amplitude modulated with various amplitude and bandwidth signals at various frequencies from the carrier. The undesired modulations are impressed on the carrier at the prime system oscillator, the rectenna pilot-beam transmitter, in the propagation medium, and within the trantenna. Figure 2-1 shows a simplified block diagram of the pilot tone — power beam electronics chain, with the various noise modulation sources identified. We shall discuss each of the spectrum contributors or modifiers in turn, beginning with the prime carrier reference oscillator.

B. THE PILOT BEAM TRANSMITTER

The origin of the trantenna RF power signal is the pilot transmitter basic frequency reference, located at the rectenna. The pilot signal or signals are first synthesized from the reference oscillator. They may then be purposefully modulated for antijamming protection or to prevent spoofing. Then they are transmitted to the trantenna subarray receivers, compared with a local reference, phase conjugated, frequency translated, and eventually transmitted back toward the rectenna at a much higher flux-density level. At each step along the way, the various electronic processes modulate the carrier and thus determine the ultimate radiated power-beam signal spectrum.

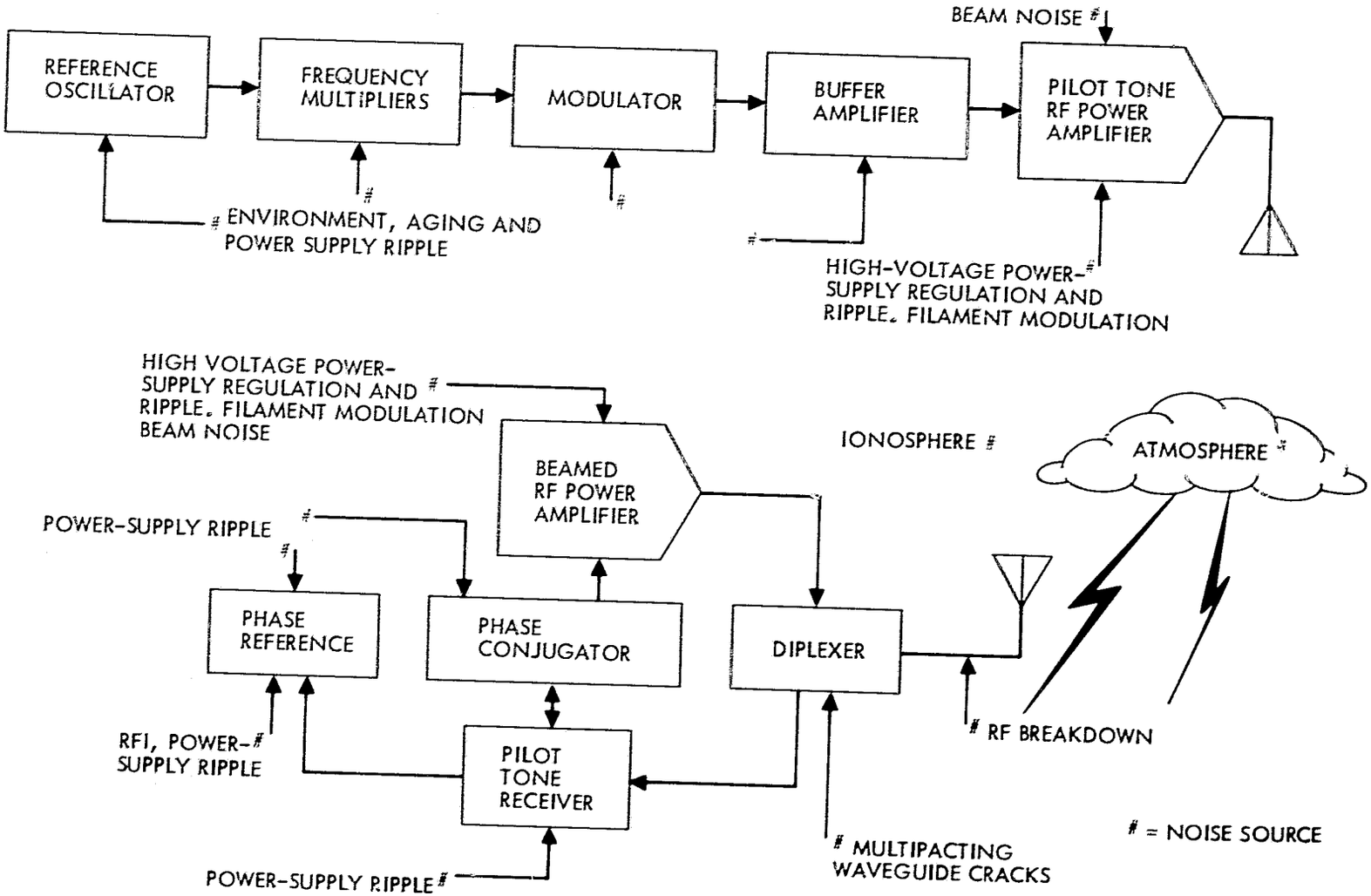

Figure 2-1. Pilot Tone-Power Beam Block Diagram

The primary oscillator is subject to a frequency uncertainty that is characterized by the Allan Variance (Reference 2-1). The primary oscillator sets a lower bound on the degree of monochromaticity of the reference signal or pilot-beam signal. For a hydrogen maser oscillator, the variance is typically a few parts in 10^{13} for an averaging time period of 1 second.

The system oscillator is usually at a low frequency, and must be multiplied and/or mixed with other frequencies derived from the basic oscillator in order to synthesize the desired pilot-tone frequency or frequencies. Monitor or command telemetry may then be modulated on the carrier, before buffering (isolation amplification level-setting) is performed in an intermediate-level power amplifier to the final power amplification in the pilot-signal transmitter output stage.

The close-in spectral characteristics of the low-power-level electronics signal may be determined in part by the ripple- and noise-filtering in their power supplies. This is because of the resulting amplitude or phase modulation (AM or PM) arising from rippling bias voltages applied to nonlinear devices with inadequate bypassing at the device terminals. Also, the power amplitude whose high-voltage power-supply is controlled by feedback regulation through comparison loops may have low frequency components of sufficient amplitude to result in low-level pilot-signal carrier modulation.

The ac filament current or inadequately filtered, dc-powered filament current in power amplifier tubes can produce low-level modulation close in to the carrier. Bifilar-wound filaments will reduce the modulation index. Reference 2-2 gives the result of measuring the incidental phase modulation of a 400 kW CW, S-band klystron. The peaks of the 400 Hz power supply ripple modulated the carrier to yield sidebands 67 dB below the carrier (dBc) at the supply fundamental, and -75 dBc at the second harmonic for an ac-powered filament. The modulated sidebands were -63 dBc for 400 Hz ac-filaments on a 100 kW, S-band klystron.

Inadequate filtering of various frequency components in the synthesis process may also result in undesired or spurious modulation of the pilot signal(s). Additionally, the shot noise in the pilot-signal power amplifiers will result in low-level modulation of the carrier. Figure 2-2 shows a concept curve of the spectrum of a power-amplified pilot-beam signal. The drawn curve is intended to show the various regions of the spectrum that are influenced by the supporting equipment as well as by the power converter device itself.

C. THE PROPAGATION MEDIUM

Once the pilot signal leaves the rectenna, it is subject to additional amplitude and phase modulation generally associated with disturbed weather conditions (Reference 2-3). The ionosphere striations (if the signal path includes the ionosphere) and disturbed weather atmosphere effects such as lightning and severe weather cells can induce phase and amplitude fluctuations due to multipath propagation. Also, the dynamics of the situation can lead to spreading of the received frequency spectrum

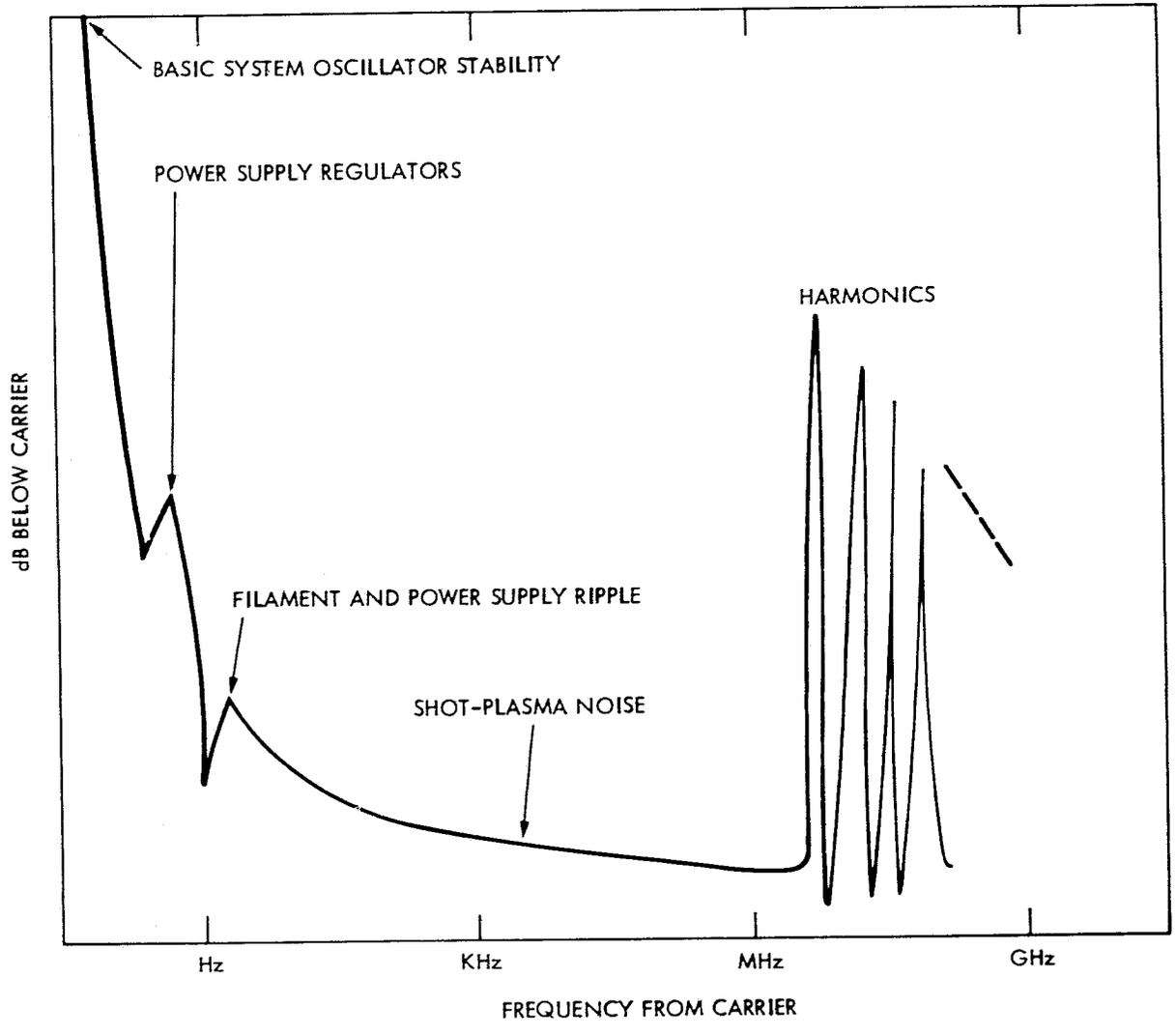

Figure 2-2. Generalized Spectrum of a Power-Amplified Signal

at the trantenna receivers. Ionosphere-caused Faraday rotation can lead to long-term AM components unless the polarization variations are tracked or otherwise compensated.

Nonlinear mixing of high-flux-density-level signals traversing the same nonlinear region of the ionosphere can potentially lead to transferred modulation.

D. THE TRANTENNA

The RF power amplifiers in the trantenna of a retrodirective phased array are to be provided with a phase-controlled RF input carrier derived from the phase conjugation operation. The phase conjugator output is obtained from the subarray-received pilot signal and the common phase reference distributed to each subarray. Thus, the near-in spectrum characteristics result from both the stability or instability of the received pilot beam and the phase reference distributed on the trantenna. Both signals may be fundamentally derived from the basic oscillator of the rectenna pilot-beam transmitter.

The trantenna signal-processing electronics used for amplifying, mixing, multiplying, level setting, and filtering, may also contribute to the resulting power signal spectrum. Power supply ripple and noise filtering and regulation along with circuit decoupling are critical design parameters in the trantenna as well as in the rectenna equipment. If phase-locked loops (PLL's) are used for performing the phase conjugation operation, then the resulting output signal may also possess near-in characteristics that are a function of the PLL voltage controlled oscillator and the loop low-pass filter. In fact, PLL's within the trantenna subarray receivers may remove or minimize some of the undesired rectenna pilot-beam transmitter and atmosphere or ionosphere induced modulation. Also, locked loops around the final power amplifiers that compare the output-radiated RF signal with a desired clean low-level reference may be employed to minimize, where possible, some of the ripple modulation in the ultimate radiated signal.

E. THE DC-TO-RF CONVERTERS

This section of the report contains the first of the experimental measurements. For both noise and harmonics, it will first discuss background information, and then in each case will present and discuss the actual measurements.

1. Harmonics

The process of bunching charged particles or depletion regions in an RF power amplifier, which is necessary to yield high-power and high-efficiency output, also produces current wave-shapes that are rich in harmonics. The effective coupling impedance presented by the output circuit at the harmonic frequencies determines the level immediately at

the device output. From there, the resulting harmonic energy is propagated via multiple modes through transmission lines to the designed filters and subsequently to the power distribution assembly before being finally radiated. The resulting transfer impedances and propagation losses between the device output and the antenna are very difficult to calculate, or even to measure. This is because of the very large number of permitted propagating modes, and the complex conversions at various obstacles and direction changes within the guides. A section of WR-430 waveguide operating at a fundamental frequency of 2.45 GHz has 8 possible modes through the second harmonic, 18 for the third, 29 for the fourth, and 48 possible propagating modes for the fifth harmonic (Reference 2-4).

Meaningful measurements (that are repeatable) of harmonics from a dc-to-RF converter can only be made with a single-mode coaxial output transmission line and a broadband load, or with a multiple-apertured waveguide probe and power-summing analysis system (Reference 1-6) for very-high-power devices. Figure 2-3 shows such a device, which was used to determine harmonic energy from up to half-megawatt continuous wave (CW) klystrons at S-band.

2. Harmonic Measurements

Figure 2-4 shows the representative measured harmonics from unfiltered Class C operation transistor amplifiers, a 2-kW magnetron, 100- and 400-kW CW klystrons, and a 20-kW CW 5K70SG klystron for two different tuning conditions. Linear operation can reduce the harmonic levels as compared with saturated operation, but at the expense of decreased efficiency and increased sensitivity to operating parameter changes.

3. Noise

The noise power output is specified in terms of the power density in a 4 kHz bandwidth in order to relate to the approximate width of a voice frequency channel for telephonic communications. Since power transmission must share the RF spectrum with communications services, this permits the direct comparison of the effects of interference by the power beam noise in any other communication band of frequencies away from the RF power beam frequency or assigned channel, such as the ISM band at 2450 $\pm$ 50 MHz.

4. Noise Measurements

Figure 2-5 shows the noise spectral power density output from klystron and magnetron RF power amplifiers. The broad band curve is drawn through a scatter plot of measured data on magnetrons, transistors, and klystrons at JPL and from other sources, as listed in the Bibliography. The individual devices' characteristics will vary as a function of tuning, saturation, output impedance, etc. The plotted curve is pessimistic in that representative conservative or worst case high

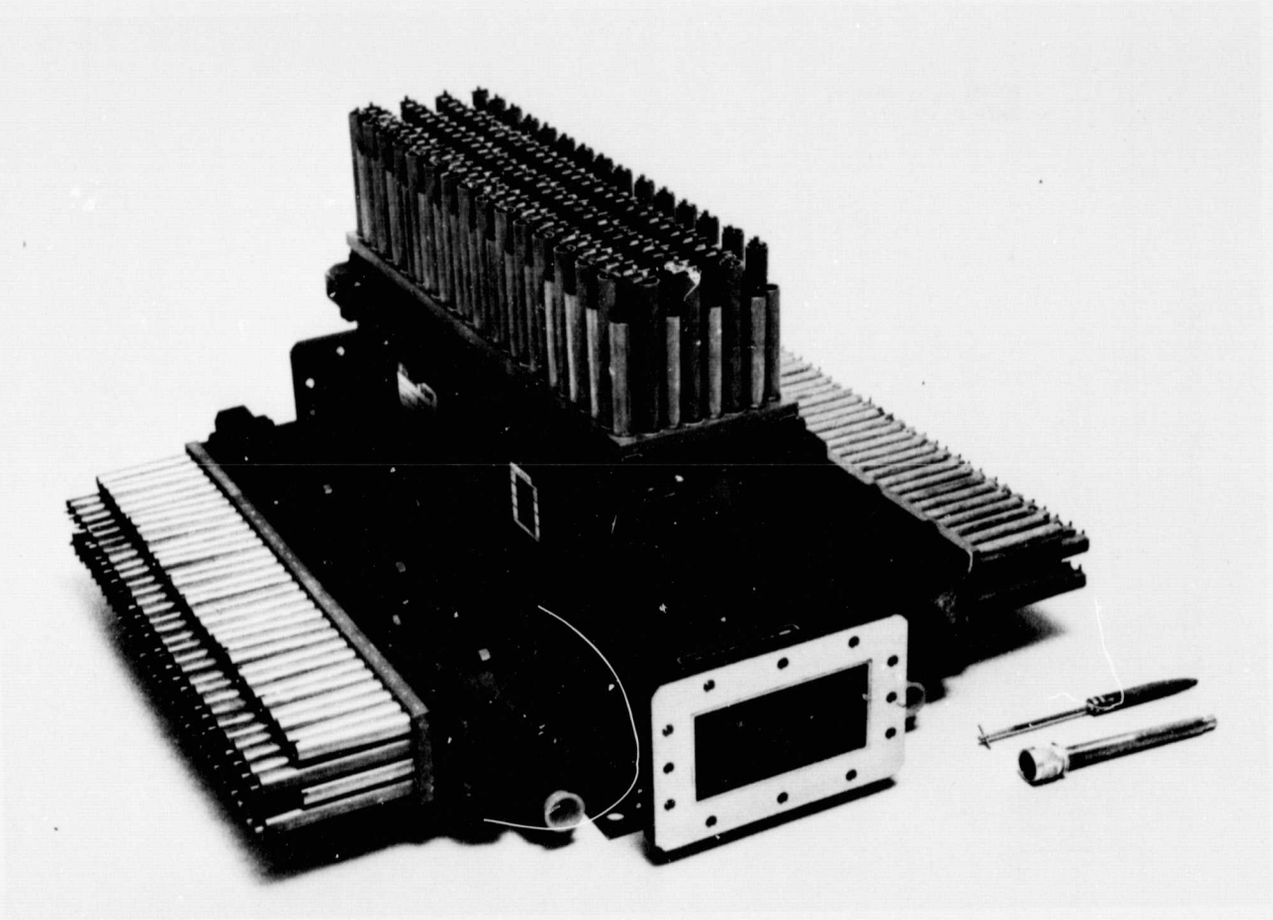

Figure 2-3. Multiapertured, Multimode Waveguide (Porcupine) Assembly

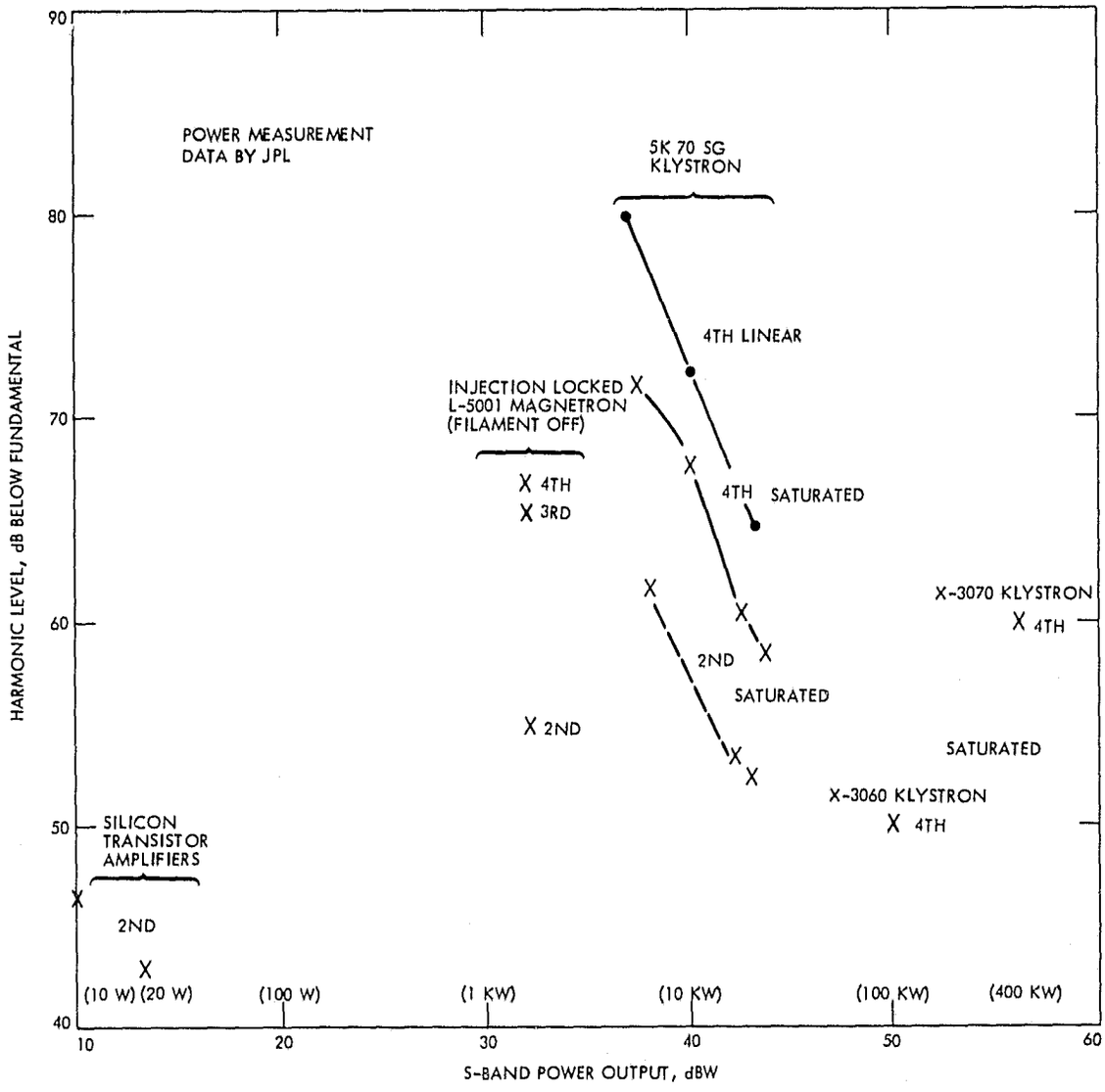

Figure 2-4. Dc-to-RF Converter Harmonics

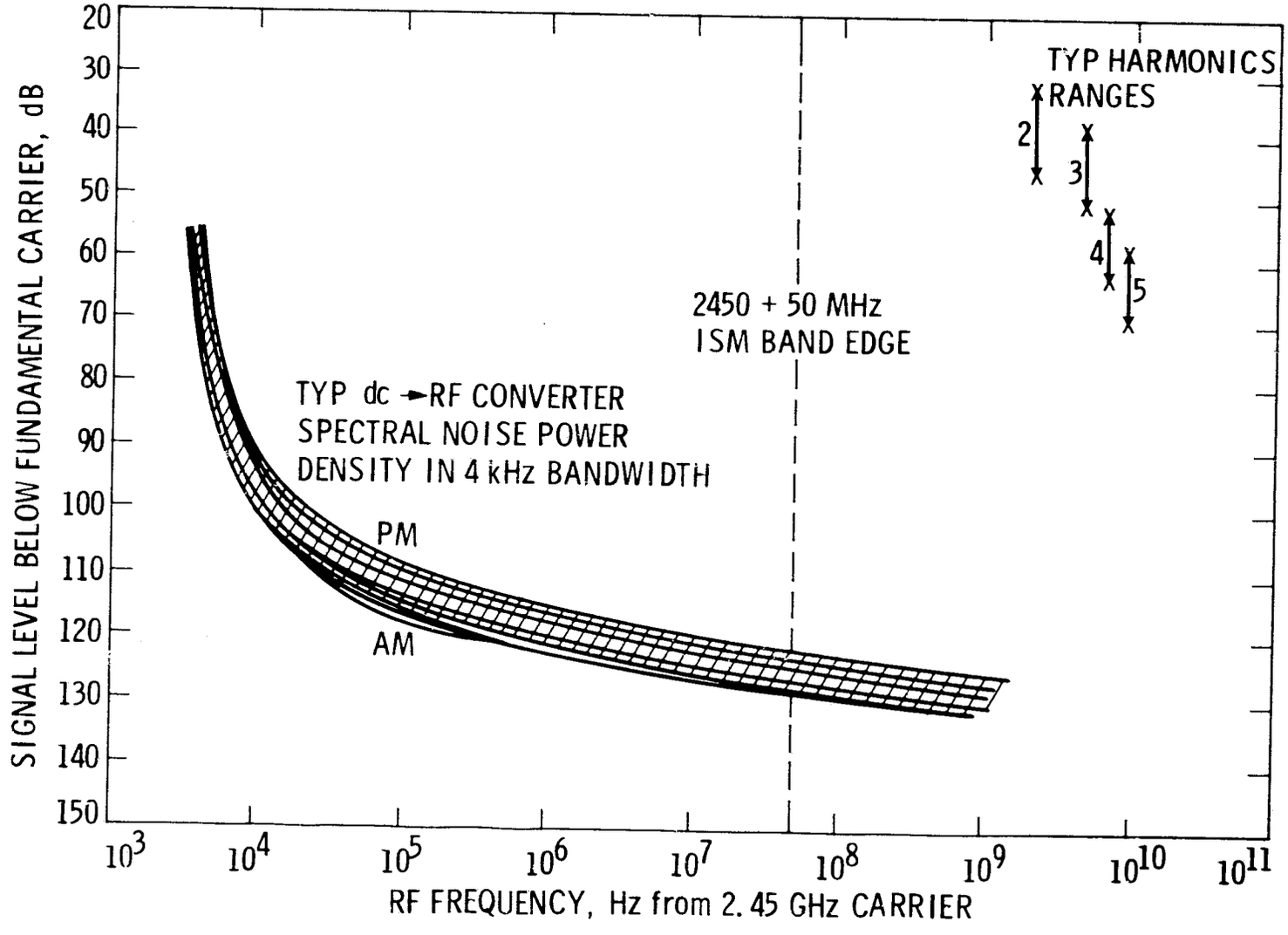

Figure 2-5. Noise Spectral Power Density, Dc-to-RF Converters

noise data is shown. Selected good performers and devices optimized for low noise performance are up to 40 dB better at the ISM band edge.

It should be noted that the klystron produces an output band of noise regardless of whether there is RF modulation on the beam of electrons streaming from cathode to collector. As the beam of electrons crosses the output gap, RF voltages are induced in the output waveguide due to amplified shot noise and space-charge spreading of the beam. The noise power output is modeled as if the klystron were an amplifier with a noise figure of between 35 and 45 dB (Reference 1-7); that is, the noise power per Hz is three or four orders of magnitude greater than if the device were simply a black body at 290K. In a 4 kHz band, the noise power would be -174 dB below a milliwatt in a one Hertz bandwidth (dBm/Hz) + 36 dB (4 kHz) + 40 dB, or -98 dBm. Thus, for a 70 kW-output klystron, the noise power far away from the carrier is -176 dBc in a 4 kHz bandwidth, with no RF drive applied. When RF drive is applied, however, the noise power increases by 50 to 60 dB, as shown in Figure 2-5.

F. PASSIVE DEVICES

In addition to the active devices previously discussed, the normally passive components such as waveguides or other transmission lines and interconnects can contribute RF noise or undesired signals to the beamed power output radiated spectrum (Reference 2-5). Sharp obstacles, loose objects, and microcracks can yield discharge arcs in high power-density situations. Gaps in waveguide junctions may be due to improper manufacture, assembly, or operations wear (repeated thermal or other structural resonance cycling) with inadequate or improper maintenance or repair.

The microdischarges reported in Reference 2-5 produce broadband noise whose peak levels can cause temperature changes of 10^2-10^3 K in low-noise receivers with predetection bandwidths of 1 MHz and post-detection smoothing of 0.1 to 0.3 sec. This indicates noise power spectral densities in a 4 kHz bandwidth of the order of -130 dBm.

Nonlinear (oxide) junctions formed in aluminium or in composites can yield intermodulation products (IMP) if more than one RF signal is present (for example, the simultaneous pilot and power beam signals, or communication, telemetry, and command RF signals). Example intermodulation product gains are given in Reference 2-5 and depend upon the power level and the type of nonlinearity. A loose object in a waveguide carrying 70 kW can produce a third-order intermodulation product conversion efficiency of -65 to -70 dB.

A more serious RF noise generator is the RF breakdown of the ionization variety in the earth's atmosphere, or multipacting if the trantenna is located in the hard vacuum of deep space (Reference 2-6). One application of beamed RF power that has received much study (Reference 2-7) is the proposed Satellite Power System (SPS). The large discharges are definitely a threat to the equipment safety, in addition to generating copious noise, and thus must be quickly extinguished by protective devices. Figure 2-6 shows permissible levels of radiated

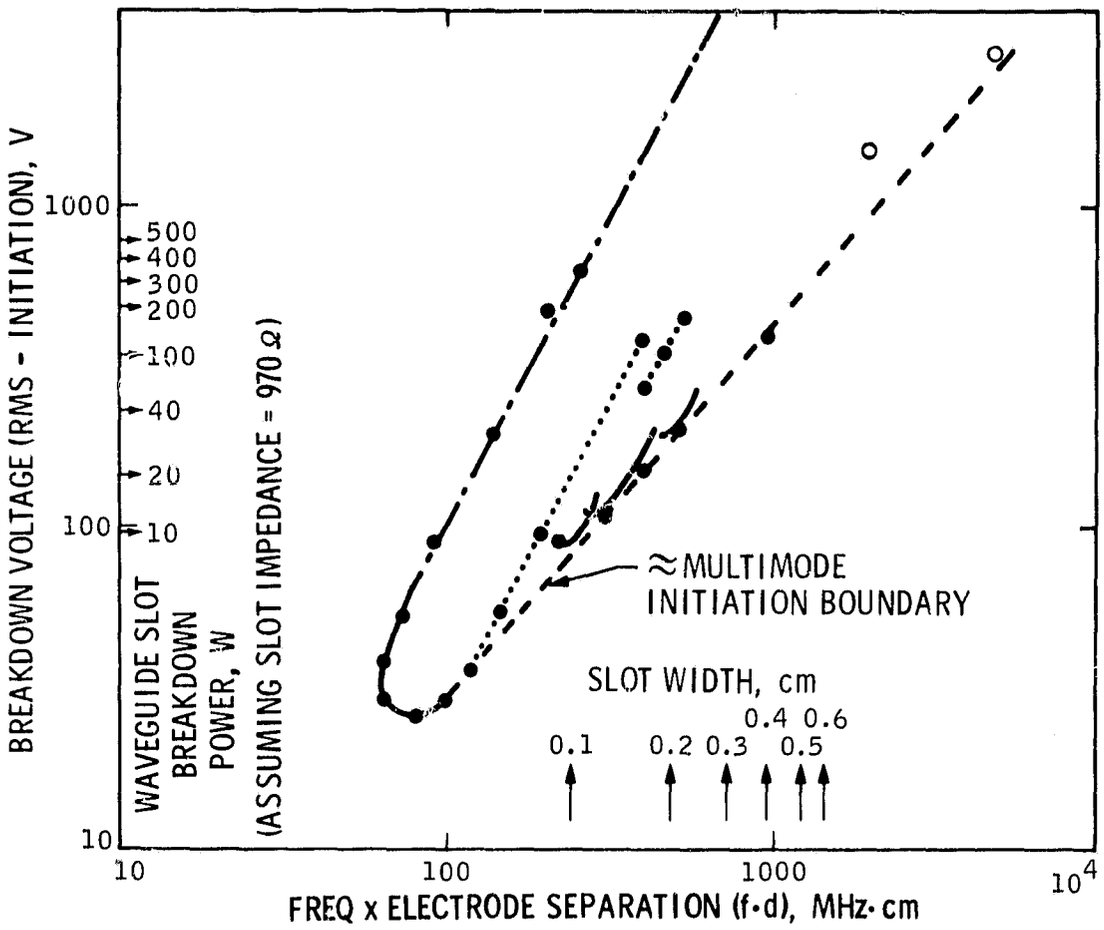

Figure 2-6. Slotted Waveguide Multipacting RF Breakdown

power from various-width waveguide slots under which 2.45 GHz RF radiation will or will not induce multipacting breakdown in a very hard vacuum. The power levels for preventing ionization breakdown are particularly lower for the very critical altitude range around 45 km in the earth's atmosphere. Otherwise, for ground-based trantennas the permitted radiated levels are much larger.

The power level and directions with which these undesired radiations are broadcast are dependent upon where in the RF chain the disturbance is generated. They are also a function of the transmission line configuration and the transformed impedance presented by the ultimate RF radiator. Figure 2-7 shows the transmitting phased array components and their characteristics that affect the radiated fundamental, noise, and harmonics. The antenna pattern characteristics are discussed in the next section.

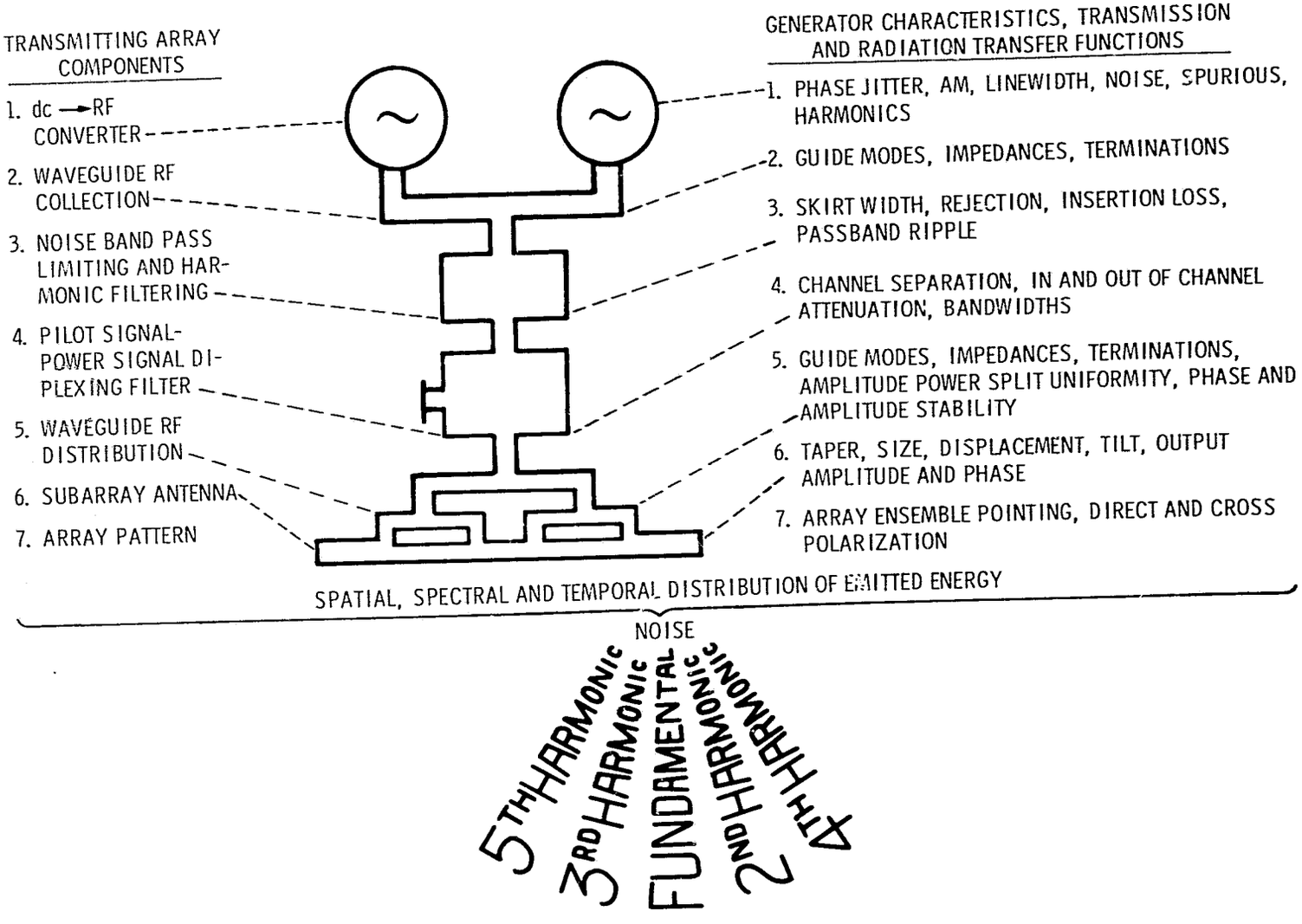

Figure 2-7. Transmitting Phased Array Charact · istics and Components That Affect Emissions

SECTION III

TRANTENNA EMISSION PATTERNS

The normal-mode or standard maintained trantenna-emitted RF radiation distributions will be presented and discussed, in addition to patterns resulting from degraded modes. Both the fundamental frequency and harmonic frequency patterns will be covered.

A. NORMAL FUNDAMENTAL PATTERN

The antenna pattern of the RF-power-transmitting active retrodirective array (ARA) at the fundamental frequency is determined, at the observing point of interest, by the integrated sum of the contributions to the electric field from the elemental phase and amplitude distribution of RF currents across the entire ARA aperture. The foregoing statement means that the ARA antenna pattern is not only a function of the aperture distribution, but is also a function of the position and distance from the ARA. Whereas the essential features of the pattern (beamwidth, sidelobe level, and null position) are nearly fully developed at a range from the aperture of twice the diameter squared divided by the wavelength ($2D^2/\lambda$), the difference in peak gain between the normal far field distance of $2D^2/\lambda$ and infinity is .04 dB or 1%, which is not inconsequential for a high-efficiency, high-power transmission system, working at long range. For a beamed power transmission system that must operate over a variable range, the pattern will vary as a function of range and angular direction from the trantenna.

The trantenna pattern is also a function of the maintenance of the ARA. Attrition or malfunction of power amplifiers or pilot-beam receivers varies the elemental phase and amplitude contributions to the final pattern. On the Earth, frost-heaving of ground, or in space, station-keeping or attitude-control variations of spaceborne trantennas, can cause changes in the main beam pattern and sidelobes and grating lobes due to varying phase distributions with respect to the rectenna or the observer's position. The opening or enlargement of cracks between differentially deflected subarrays, due to mechanical stresses, leads to the appearance or increase in amplitude of grating lobes in the pattern at the fundamental frequency. Blocking of radiation from the trantenna aperture by absorbing or scattering objects such as leaves, trash, dust, melting snow, etc., can lead to undesired fundamental frequency patterns. Severe blockage reflections can lead to RF breakdown in some of the trantenna subarrays with seriously distorted patterns and radio frequency interference (RFI) consequences. Therefore scheduled and unscheduled maintenance must be planned for trantennas, and must be appropriate for the expected environment.

The trantenna pattern may vary with the amount of prime power available to the transmitting array dc-to-RF converters. For example, if the power converters were linear, then a change in the prime power voltage amplitude would only result in a change in the absolute magnitude of the fundamental power pattern. However, as most designs will

employ saturated dc-to-RF conversion devices in order to promote some degree of insensitivity to operating conditions, the ARA aperture amplitude distribution will change due to different degrees of saturation and thus to differing power output changes with beam voltage changes. The changes could be avoided by imposing severe voltage regulation, but this would lead to reduced overall efficiency, increased weight, and increased cost.

Most of the truly random changes in the antenna aperture amplitude and phase distributions will, to first order, not seriously affect the location of the peak of the beam — that is, the pointing of the ARA. Generally, a well-correlated failure across many subarrays, or another nonstandard operating condition affecting a large fraction of the subarrays, is required to yield a phase taper across the ARA aperture that would result in a consequential misdirection of the beam.

Figure 3-1 is a block diagram of some of the factors affecting the SPS microwave power transmission level and antenna pattern shape. Table 3-1 lists some of the factors affecting the resulting flux density distributions around the Beamed Power System. The resulting field strength at any point is the vector sum of all the field contributions from the original source as well as scattered and rescattered contributions, even under normal circumstances.

B. DEGRADED MODE FUNDAMENTAL FREQUENCY PATTERNS

Degraded modes are considered to occur whenever the permissible phase and amplitude design tolerances in the aperture are exceeded. Such conditions may exist during turn-on or turn-off, depending upon how the functions are mechanized. Inadequate maintenance, excessive converter failures, or degraded signal-to-noise ratio in the pilot-beam receivers could produce nonstandard fundamental frequency patterns. Causes could range from aging of equipment, to interfering signals, to nonlinearities of consequence in the propagating medium.

As previously mentioned, for aperture errors that are truly randomly spread across the ARA, the beam remains pointed at the pilot-signal transmitter located at the rectenna. Where the errors are strongly correlated, the beam may be mispointed or misshapen. Random errors cause the peak beam intensity to decrease, the sidelobes to increase in amplitude, the beamwidth to increase, and the nulls of the pattern to be filled in.

For correlated errors, an equivalent linear phase gradient across the aperture that results in a peak phase error of half a wavelength between the edges of the ARA, will produce an electronic beam scan of half the array beamwidth.

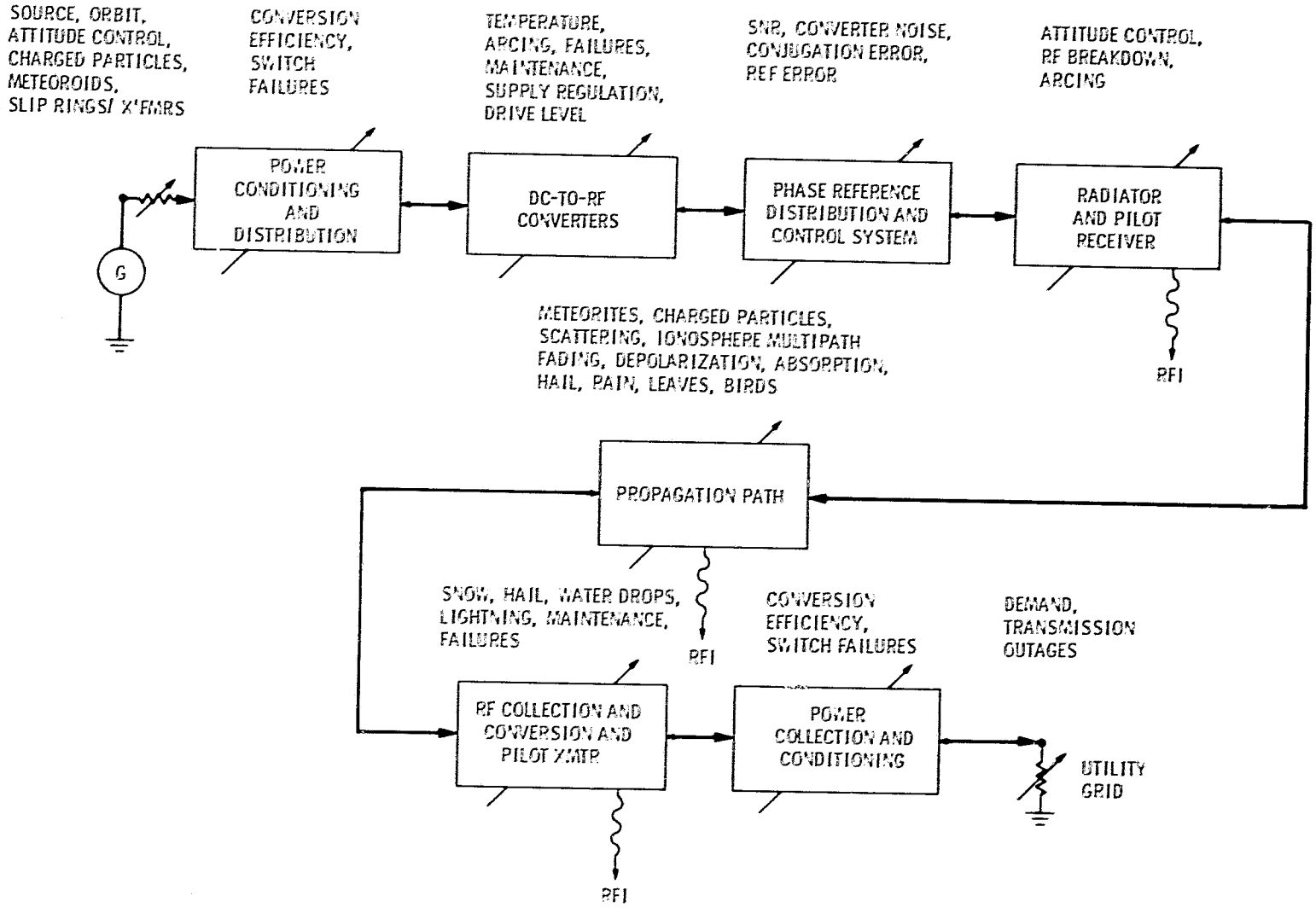

Figure 3-1. Factors Affecting Transmission Level and Pattern Shape

Table 3-1. Factors Affecting Flux Density Distributions

I.	Peak Flux Density
	1. RF Power
	2. Range
	3. Array Diameter in Wavelengths
	4. Propagation Effects
	5. Phase Quality
II.	Beamwidth
	1. Array Diameter in Wavelengths
	2. Aperture Taper
	3. Phase Quality
III.	1st Sidelobe Level
	1. Aperture Taper
	2. Phase Quality
IV.	Minor Sidelobes Levels
	1. Phase Quality
	2. Amplitude Errors
	3. Subarray Size
	4. Element Pattern
V.	Beam Pointing
	1. Phase Quality
	2. Retrodirective Receiver Signal-to-Noise Ratio
	3. Array Mechanical Pointing
VI.	Rectenna State
	1. Load Condition
	2. Maintenance
	3. Configuration

C. TRANTENNA HARMONIC PATTERNS

1. General Discussion

Once the harmonics are generated in a dc-to-RF converter, the undesired RF may be radiated directly by an integral antenna that may be a portion of a solid-state converter and its filter; or else, the undesired RF may be transported to the radiating antenna element with waveguide or other low-loss transmission lines. The measured results presented here deal principally with the concept approach for the ARA of employing rather large-power-level converters whose outputs are distributed with waveguides to slotted waveguide ultimate radiators. Hence the following discussion is principally waveguide oriented.

Figure 3-2 shows the principal waveguide elements for power distribution (input guide, feed guide, and radiator guide) and their arrangement for a subarray radiator. The directions and amplitudes (patterns) of the harmonic radiations that issue from the slotted waveguide subarray antenna are functions of the internal current distributions within the various guides. The current distributions result from the multimode propagation permitted at the harmonic frequencies because of their short wavelengths. Thus, each bend or other obstacle or transition within the guides changes the relative proportion and phases of the harmonic power in the various modes. Also, the resulting harmonic patterns are a function of how the harmonic currents are introduced (coupled) into the guides from the converters. For example, the measured difference in average gain level for the harmonics radiating from a stick of S-band waveguide fed from a long, smooth, tapered waveguide transition was about 10 dB higher than the same waveguide stick harmonic patterns when fed with an abrupt coax-to-waveguide transition.

The expected pattern of the radiation from the slotted waveguide antenna at the harmonic frequencies is a series of randomly spaced grating lobes within a bounding envelope. The shape of the envelope is that of the pattern of an elemental radiating unit (slot) of the array at the harmonic frequency. Even the elemental slot harmonic pattern is multidimensional due to the fact that the patterns are a function of the point of excitation of the harmonic current within the slot. Due to construction tolerances and dissymmetries within the feeding structure, the various slots will be differently excited and thus will radiate with differing patterns. The fabrication tolerances and the multimode propagation within the guides will lead to random phasing, and due to multiple VSWR reflections, there will be random amplitudes of excitation at the various slots also. Nevertheless, the regular spacing of the slots will tend to produce somewhat regular angular width lobes of radiation whose amplitude and spacing vary randomly. And, although the approximate lobe angular width may be calculated, the resulting amplitude or the absolute gain of the harmonic pattern is not readily amenable to direct calculation. Hence, we set out to make some absolute gain measurements of harmonic radiation patterns from a representative beam power transmitting slotted waveguide subarray. Given a model of the propagation losses and relative proportions of energy within the various modes in the guide, one could employ Monte Carlo simulation to assign random phases to the slot radiators and calculate statistical patterns, given also the elemental slot harmonic patterns.

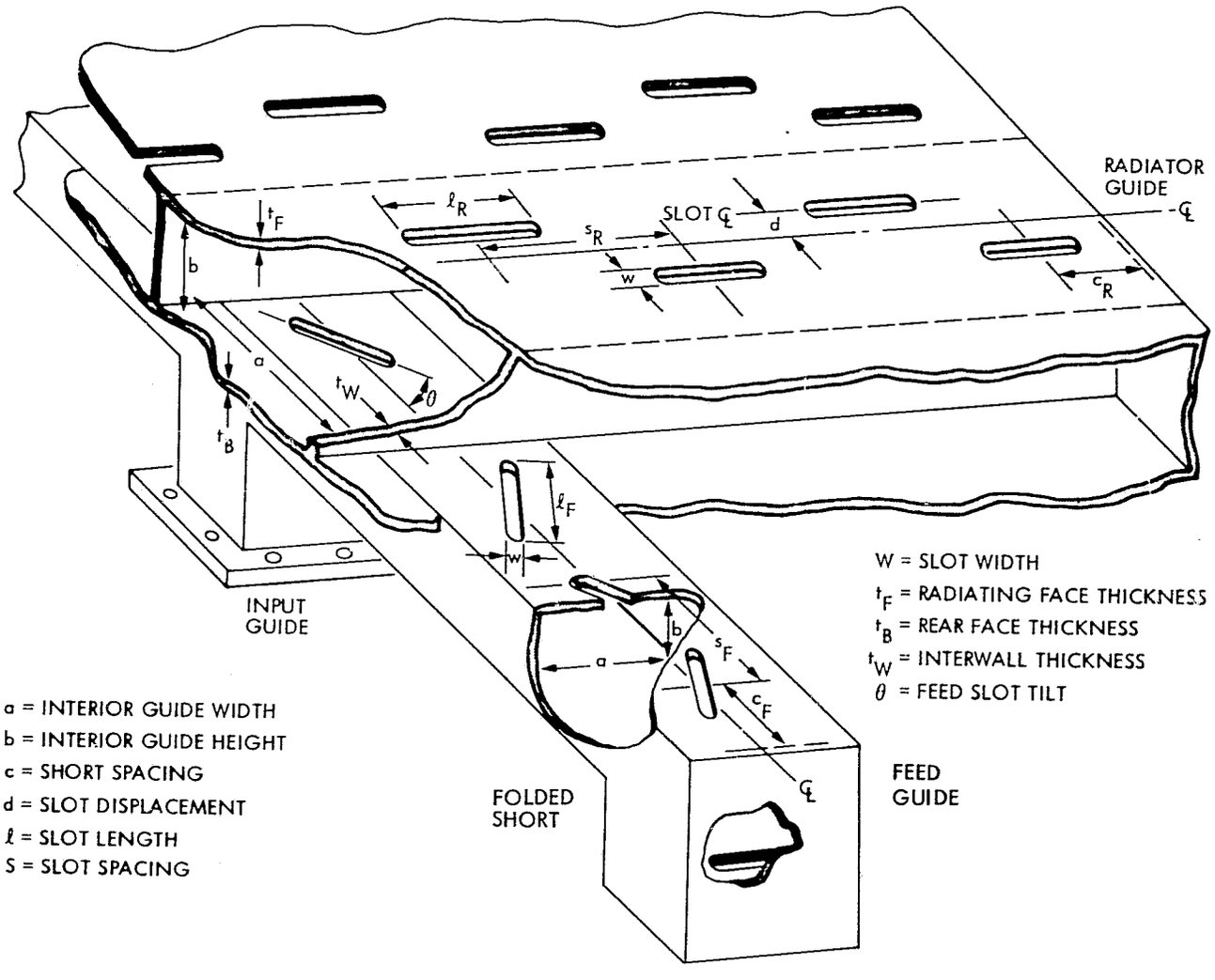

Figure 3-2. S-Band Slotted Waveguide Subarray

2. Measured Patterns

Figure 3-3 is a composite chart consisting of various measured patterns produced by the six-wavelength-square, 64-element (8 waveguides with 8 slots each) slotted subarray radiator shown in Figure 3-4. The patterns are E- and H-plane and crossed polarized radiation (XE and XH) for the fundamental, second, third, fourth, and fifth harmonics, when measured at an abrupt coax-to-waveguide transition connected to the input waveguide. The transition is tuned only at the fundamental frequency and thus probably provides an unknown degree of mismatch desirable for the harmonics. The average (peaks are 6 dB higher) gain of the third and fourth harmonics is 50 dB below the fundamental peak gain. The average of the second and fifth harmonics is 65 dB below the fundamental peak gain. An envelope pattern bounding all the harmonics (not all shown in the figure) was eyeball-fit with a $\cos^{1.4}\theta$ pattern, as shown. The cross-polarized fundamental radiation is about 50 dB below the desired polarization radiation. The techniques employed in measuring and calibrating the harmonic patterns are discussed in the Appendix. The family of $\cos^{x}\theta$ patterns was selected to bound the harmonic patterns because they adequately model elemental radiator, low gain pattern shapes. Randomly positioned, narrow grating lobe (harmonic) patterns would be expected to be contained within such $\cos^{x}\theta$ envelopes.

Table 3-2 shows the differences in measured absolute gain between the harmonics radiated from the 8-slot waveguide stick and the total 8-stick subarray. The differences are thought to be principally due to the additional transmission line, and to coupling losses in propagating the harmonics through the feed guide. The measured radiated signal levels include VSWR reflection losses at the slot aperture as well as conductor losses inside the guides. The aperture reflection losses may be similar in the two cases, but the losses are larger because the feedguide aperture is in series with the radiating aperture. Thus, additional waveguide junctions used for power dividing or combining may offer added harmonic insertion loss filtering.

The harmonic frequency patterns are lower in absolute gain level than the fundamental due to the random phasing of the elemental contributions from each slot. This is because of the different unplanned path lengths involved in the multimode propagation at the high frequencies in the S-band waveguide. Minor differences in construction tolerances resulting from manufacturability design requirements will assure that no two subarray antennas' harmonic patterns will be the same. Therefore, the concept of an envelope pattern bounding the essential harmonic radiation patterns is a convenient artifice to permit describing the average level of the harmonic radiation from any similar slotted waveguide subarray of the same size and with the same feeding arrangement.

3. Application of Data

In order to extrapolate the measured harmonic gain from the 64-element slotted waveguide subarray to a larger (or smaller), similar subarray fed with the same abrupt coax-to-waveguide transition and with the same internal T-junctions and feed slot coupling, the gain at the

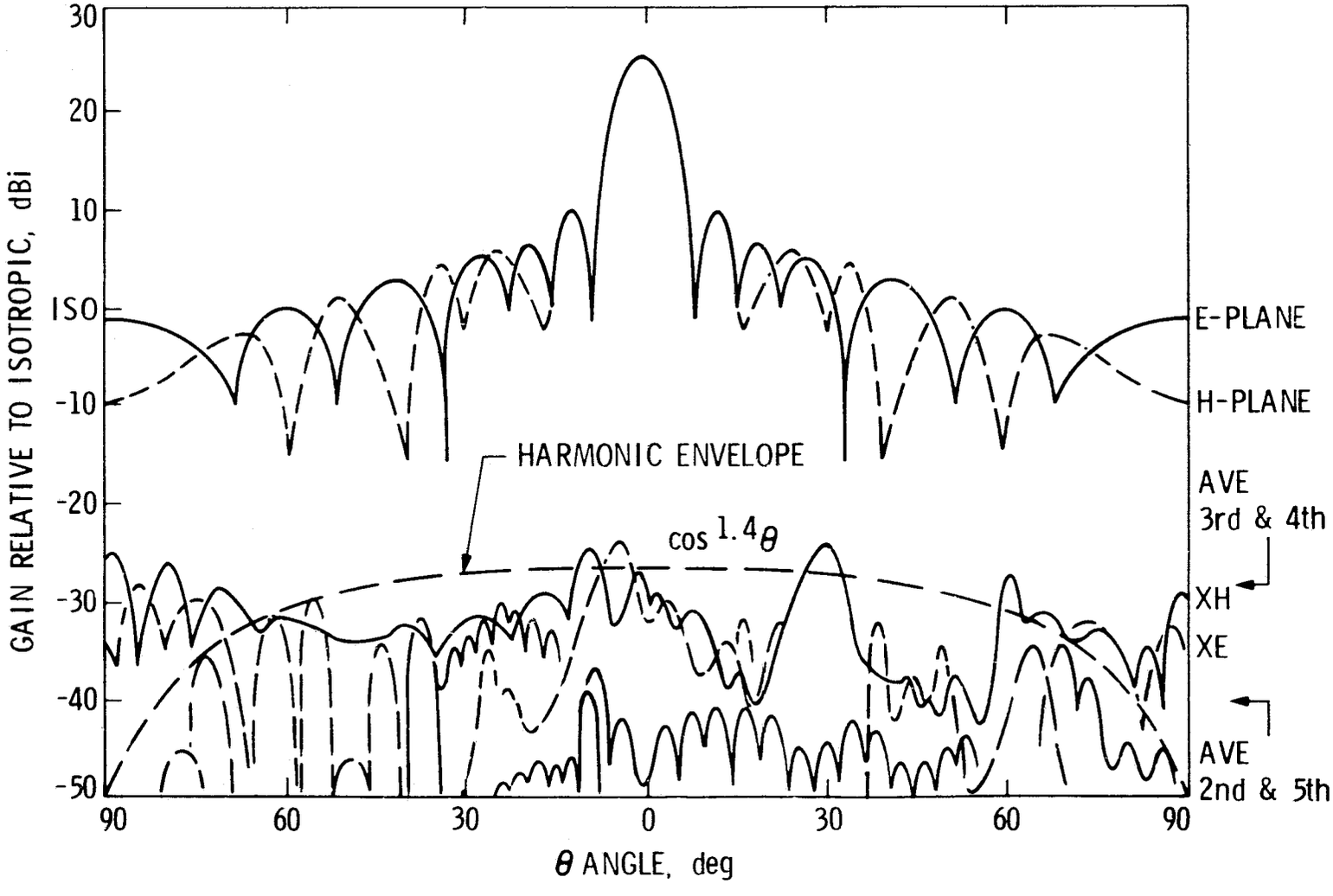

Figure 3-3. Slotted Waveguide Subarray Fundamental and Harmonics Patterns

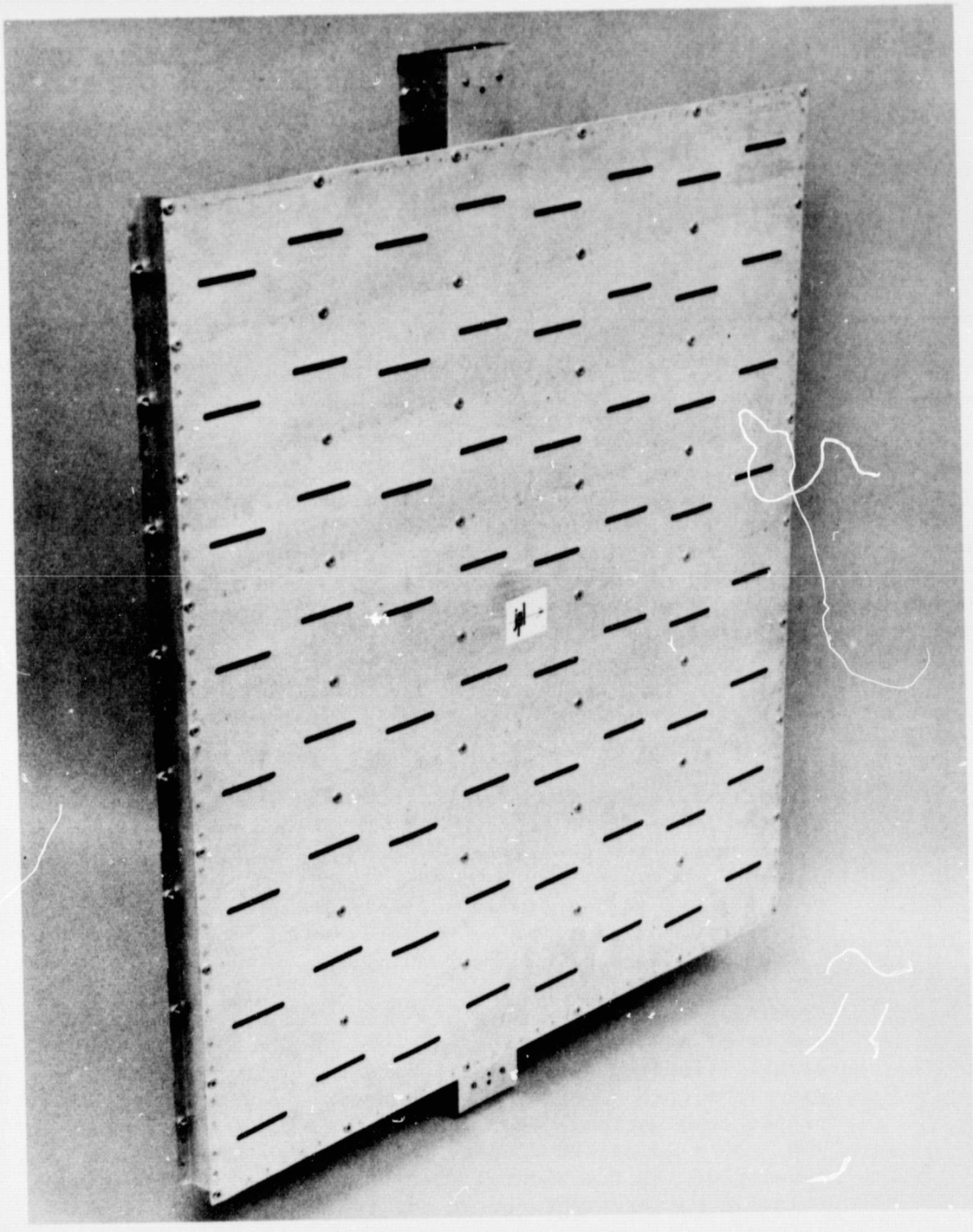

Figure 3-4. S-Band Slotted Waveguide

Table 3-2. Differences in Measured Harmonics Gains

Frequency GHz	8-Slot Stick Gain, dBi*	8-Stick Subarray Gain, dBi	Gain Difference dB
2.45	+15.31	+25.42	+10.11
4.90	-10.7	-38.8	-28.1
7.35	- 7.7	-27.3	-19.6
9.80	- 1.7	-28.2	-26.5
12.25	- 4.7	-36.6	-31.9

*dB relative to an isotropic radiator.

fundamental will increase (or decrease) by the ratio of the subarrays' area (that is, the number of slots squared) while the essentially non-coherent or large-phase-error harmonics gains will only increase (or decrease) as the square root of the ratio of the areas (that is, only directly as the number of slots). It would appear that the trantenna design to minimize the strength of harmonic radiations would favor the larger-sized subarrays.

To calculate the expected harmonic radiation level in a particular direction from an ARA employing the slotted waveguide antenna and a tube-type dc-to-RF converter, proceed as follows:

(1) From Figure 2-4, determine the harmonic level relative to the fundamental for the desired device and power level. For example, fourth harmonic, 58 dB below fundamental.

(2) From Figure 3-3, determine the gain in the direction of interest. For example, at 60 degrees off boresight, -30 dBi or 55 dB below the fundamental peak gain.

(3) Combine the above and increase the level directly by the number of subarrays in the ARA for a uniformly illuminated array. (Tapered apertures require the harmonic contribution from each subarray to be appropriately weighted for proper combination.) For example: with 200 subarrays, -58 - 55 + 23 or -90 dB net, relative to the peak flux density of the fundamental, but at an angle of 60 degrees relative to boresight and at the frequency of the fourth harmonic.

(4) Alternatively, the absolute harmonic power per subarray can be calculated and the gain relative to isotropic can be used with the spherical spreading space loss to determine the absolute flux density at the direction and range desired. That is, the power density (P.D.) at range R is given by

$$P.D. = P_h G_h / 4\pi R^2,$$

where P_h and G_h (the product of which is the effective isotropic radiated power or EIRP) are the harmonic power radiated and the gain at the harmonic frequency in the direction of interest. The gain should include the effects of the array of harmonic subarrays.

SECTION IV

RECTENNA REFLECTION AND EMISSION CHARACTERISTICS

The rectenna (Reference 1-2) is designed to collect the beamed microwave power and to convert it to dc voltage and current output. In order to perform those functions most effectively, the rectenna must be properly sized and oriented toward the incoming beam. The individual RF collecting elements must be tuned to the proper frequency. The proper magnitude of load resistance must be presented to each element according to the level of incident RF flux density. The spacing of adjacent elements and the spacing of the individual element from the reflecting ground plane must be appropriate. The RF leakage through the ground plane and its conductivity and smoothness must be satisfactory. The RF structure must be electrically balanced and the input and output low-pass filters must possess the correct cutoff frequencies and yield the correct impedance transforming properties while properly phasing the harmonic currents. Finally, the diode must switch on and off with acceptable impedance states while withstanding the high voltages, high currents, and operating temperature stresses. The above design requirements, some of which compete with each other, cannot all be achieved simultaneously. Consequently, engineering tradeoffs must be made to arrive at a satisfactory overall design. The resulting compromise design will necessarily have some small but finite reflection or rescatter of the fundamental frequency RF, and will permit some emission of harmonic energy. Currently achievable quantities are reflection less than 2% and harmonic emission more than 25 dB below the fundamental input power level. The nature, causes and character of the scattered and emitted energy under normal and degraded modes of operation are presented in this section.

A. FUNDAMENTAL FREQUENCY REFLECTION CHARACTERISTICS OF THE RECTENNA

1. General Discussion

The scattering of the fundamental frequency input RF is determined by both the physical structure (dipole array, ground plane, supports, exposed transmission lines, radome or weather protection, etc.) and the effective terminating impedance across the dipoles. Therefore, the rectenna reflection characteristics are expected to be a function of both the incident microwave flux density level and the rectenna dc load value as well as of the orientation in both azimuth and elevation of the dipoles relative to the polarization of the incoming RF wave.

A change in the design center value of either the dc load resistance, the incident RF flux density (due to amplitude or angle of incidence variations), the polarization, the frequency, or the operating temperature will result in a change in the bias voltage across the rectifying diode. The bias voltage change affects the effective capacitance of the rectifier, which causes the RF impedance presented by the dipole to the incoming RF wave to change. The net result is an impedance mismatch, which leads to reflection of a portion of the incident wave energy.

The exact character of the reflection is a function of the detailed effective impedance present at the dipole terminals and of the character of the array. For example, a short circuit at the dipole leads to the largest effective scatter cross section (Reference 4-1) of the antenna elements. Large values of resonant currents flow in the dipole arms, and the electromagnetic mutual coupling between elements is large. The plane of reflection is essentially in the plane of the dipoles. Because of physical construction tolerances and variations in electronic parameters, the phases of the RF currents radiated from each dipole are expected to exhibit a degree of randomness, which will tend to produce a smearing of the otherwise mirror-like reflection character of a short-circuited array. In general, there will be two distinct characteristics to the reflection:

(1) A "high-gain" reflection pattern with a narrow angular width directed at an angle of reflection from the array equal to the angle of incidence from the normal or boresight to the array, which is due to the preponderant character of the overwhelming short circuit reflection.

(2) An underlying "low-gain" reflection pattern caused by the effective small phase errors throughout the rectenna sub-array. In effect, the mirror will have random distortions and thus will produce a wavy image of the illuminating RF beam source.

The reflection characteristics of a rectenna with an effective open-circuit impedance at its dipole terminals is different, in that the effective scattering cross section of the antennas under these conditions is quite small. For this condition, the incident RF wave "sees" the plane of the dipoles as essentially transparent. The reflection is then determined principally by the character of the ground plane underneath the dipoles. It would be expected that, given a smooth ground plane, the "high-gain" reflection pattern or a mirror-like reflection pattern would be very predominant, with only a very small "low-gain" or wide-angle pattern due to the small shadowing of the dipoles. Again, small construction tolerances and electronic differences would result in a phase error smearing-in-angle of the dipole reflected components, as compared to the nearly uniform phase, smooth-ground plane-reflected component. In effect, a better mirror is expected for this condition. The effective scattering cross section of the open-circuited dipoles is quite small because only a very small current can be induced in the dipole arms due to the high impedance. Also, the mutual coupling to adjacent dipoles is very low because of the small currents. For intermediate values of an effective terminating impedance that is between an open and a short circuit, the rectenna is an absorber and a reflector simultaneously. The degree and character of the reflection is a function of the degree of departure of the dipole impedance from the optimum. The optimum impedance is the incoming wave impedance as transformed by the array (Reference 4-2), and the character is determined by whether the impedance is closer to a short or an open circuit condition at the dipole terminals. The composite reflected signal patterns will consist of both the "high-gain" and "low-gain" form of reflection contributions.

The resulting pattern will be a function of the relative magnitudes and phasing of the impedance mismatch and the degree of uniformity of rectifier construction and electronics parameters.

For a tightly coupled, close spaced rectenna array, the fundamental frequency reflected amplitude is expected to be quite small (Reference 1-1) when operated at the proper design conditions of incident flux density, dc load resistance, polarization match, and angle of incidence. Figure 4-1 shows the effects of various parameter variations on the magnitude of scattered power from a rectenna. A laboratory rectenna array was measured to have on axis a level of reflected power that was 27.5 dB below the incident power when properly matched (less than 0.2% reflected power).

Reflection of a portion of the incident RF energy will result when varying load demand due to normal or fault circumstances causes a dc load variation at the rectenna. Such a variation may follow when an over-voltage stressed rectifier diode presents improper effective load impedance to the dipole terminals. This reflection can also happen under conditions of higher than design-level illumination, which can be particularly acute in those designs wherein the load is tapered across the rectenna. Such conditions of excessive illumination may occur whenever the power beam is pointed off the center of the rectenna array.

For extreme cases of input RF-signal-level overloading, the excessive voltage across the diodes will generally lead to a punch-through of the expitaxial layer in the weakest semiconductor material, yielding a short circuit. This form of stress relief leads to a significant dipole impedance mismatch with consequent reflection from all elements in parallel with the faulted diode. However, this state of affairs is generally short lived, because sufficient rectenna elements in the paralleled group will survive to clear the fault by producing enough short-circuit current to fuse open the chip bond wires inside the package of the faulted diode. When this happens, the remaining paralleled elements can resume operation, and significant reflection will only occur from the open-circuited rectenna element(s).

Over-voltage stressing of the diodes can also occur under normal illumination level conditions if the effective dc load is light. For protection of the diodes in that case, a voltage-limiting scheme is required. A crowbar is very effective, but extreme. An SCR-crowbar was employed in the 34-kW-at-1.6-km tests at Goldstone in 1975 (Reference 1-2).

For the same subarray operating more nearly at its design conditions, the reflection would be a much smaller fraction of the incident flux density, because the diodes would be conducting. The pattern of the reflected fundamental for those conditions would be expected to be quite different. The effective aperture rms phase error would be much larger, and therefore the energy would be spread over a much larger range of angles. Rather, the intensity would be expected to be larger at wider angles off boresight, as compared to the low-level intensity illumination case.

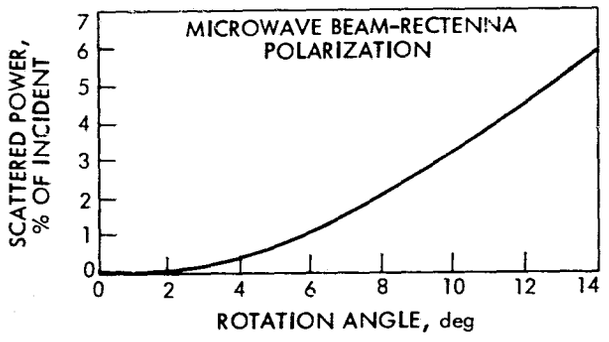

a. SOLAR STORM FARADAY ROTATION
b. SATELLITE ROTATION
c. MISALIGNED RECTENNA DIPOLES

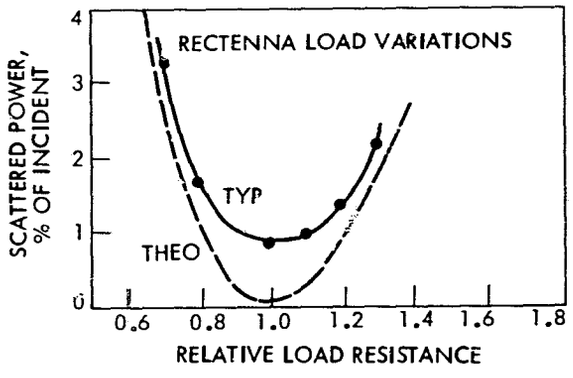

a. UTILITY DEMAND
b. RECTENNA OUTPUT COLLECTION MGT
c. RECTENNA MAINTENANCE

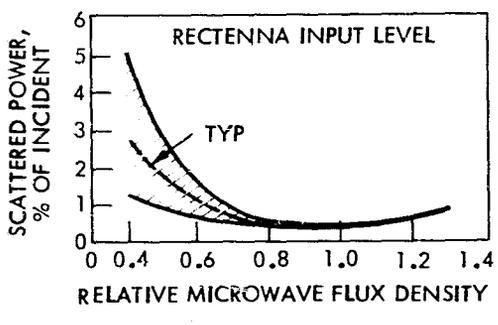

a. PROPAGATION VARIATIONS
b. TRANSMIT SUBARRAY FAILURES
c. ANNUAL SOLAR IRRADIANCE VARIATION
d. RECTENNA MAINTENANCE
e. SPACECRAFT ATTITUDE CONTROL AND STATION KEEPING

Figure 4-1. Factors Affecting Rectenna Re-Radiation RFI Levels

2. Measured Patterns

Figure 4-2 shows the fundamental and harmonic patterns measured for the shorted subarray. Details of the experimental setup and techniques are given in the Appendix. Figure 4-3 is a photograph of the rectenna mounted in a large ground plane, while Figure 4-4 shows an absorbing screen mounting. The patterns were essentially the same for either mounting of the rectenna subarray. The illuminating horn represented a compromise to permit a reasonable spread of the limited power output of about 17 watts at 2.45 GHz from a laboratory traveling-wave tube amplifier (TWTA). Closer spacing or a higher gain illuminator would permit more intense illumination, but at the expense of either more severe taper across the rectenna aperture, or greater blockage of the illuminator horn along the boresight of the array.

The essential features of Figure 4-2 are the broad angular range of the reflected fundamental frequency energy and the relatively flat top to the pattern, allowing for the diffraction around the illuminating horn and its supporting waveguide. The illuminating horn pattern is not simply mirrored in the rectenna reflection, as the beamwidth is much larger than the $\cos^6\theta$ pattern.

Figure 4-5 shows the same rectenna pattern for more uniform, but lower peak-level illumination and for 15 ohms load resistance for each 6-dipole element row. The character of the reflected fundamental radiation is quite similar to the shorted case. The power out of the array totaled 3.63 W, resulting in 21% effeciency of power transport and recovery. The efficiency is defined as the ratio of RF input power received by the illuminating horn to the dc output of the rectenna. While the subarray would normally be more uniformly illuminated and at much higher level, the recorded patterns are expected to display most of the normally operating pattern characteristics. The illumination level was changed from a very uniform 2 mW/cm^2 (80-cm illuminator spacing) to a very peaked 32 mW/cm^2 (20-cm illuminator spacing), and the scattered fundamental pattern characteristics did not change noticeably.

Higher values of load resistance tailored to each row could have achieved better efficiency (35% maximum for the 20-cm spacing case), but at the risk of losing the rectennas. The load resistance per row was decreased to 7.5 ohms (the efficiency dropped from 35% to 19.8%), also without significant change in the reflected power pattern shape.

The scattered fundamental energy from a collection of rectenna subarrays is expected to be rather broad in angular coverage also, because of the random phasing of the reflection from the dipoles, when the array is normally operating. Diffraction from the edge subarrays, shown in Figure 4-6, and multiple scatter from serrated configuration subarrays will further modify specific array rectenna patterns of rescattered fundamental energy.

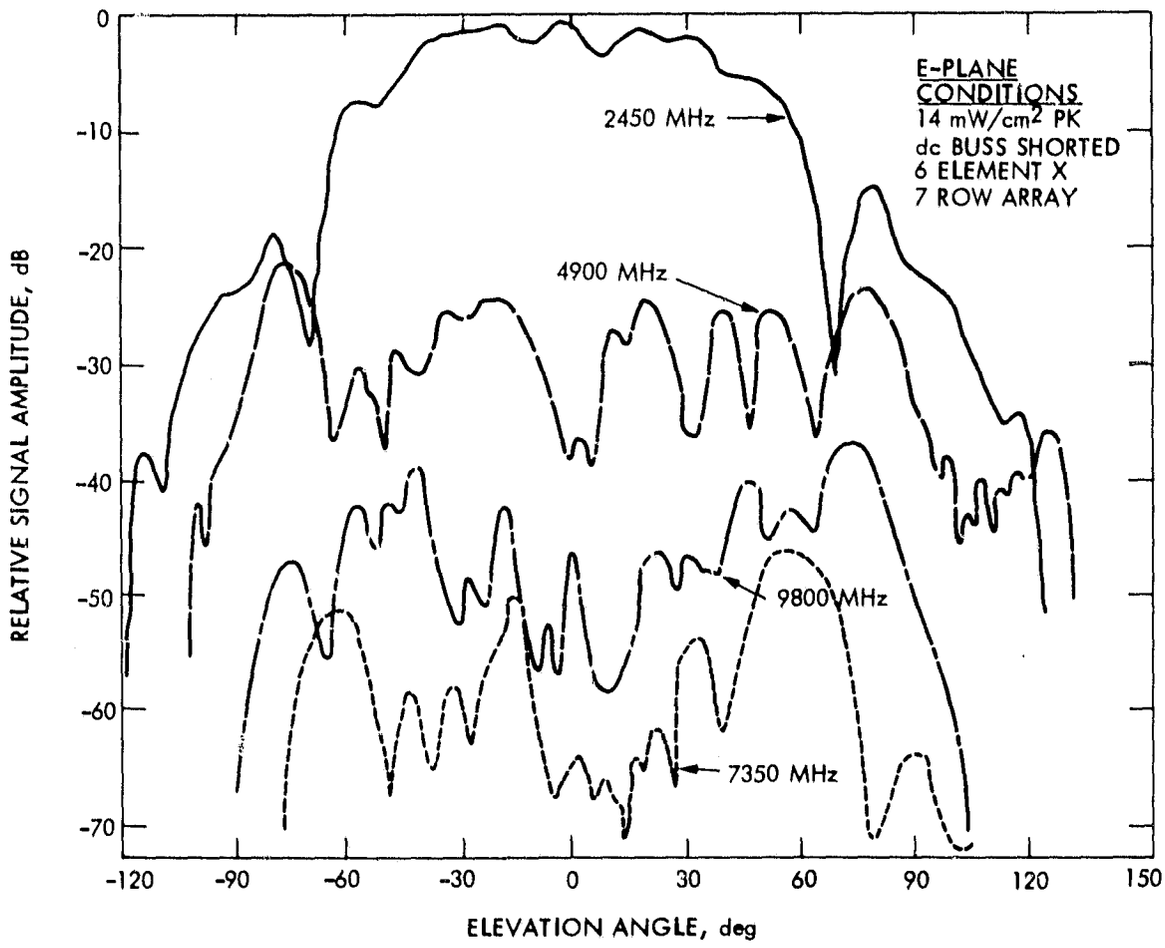

Figure 4-2. Shorted Rectenna Rescatter and Emissions

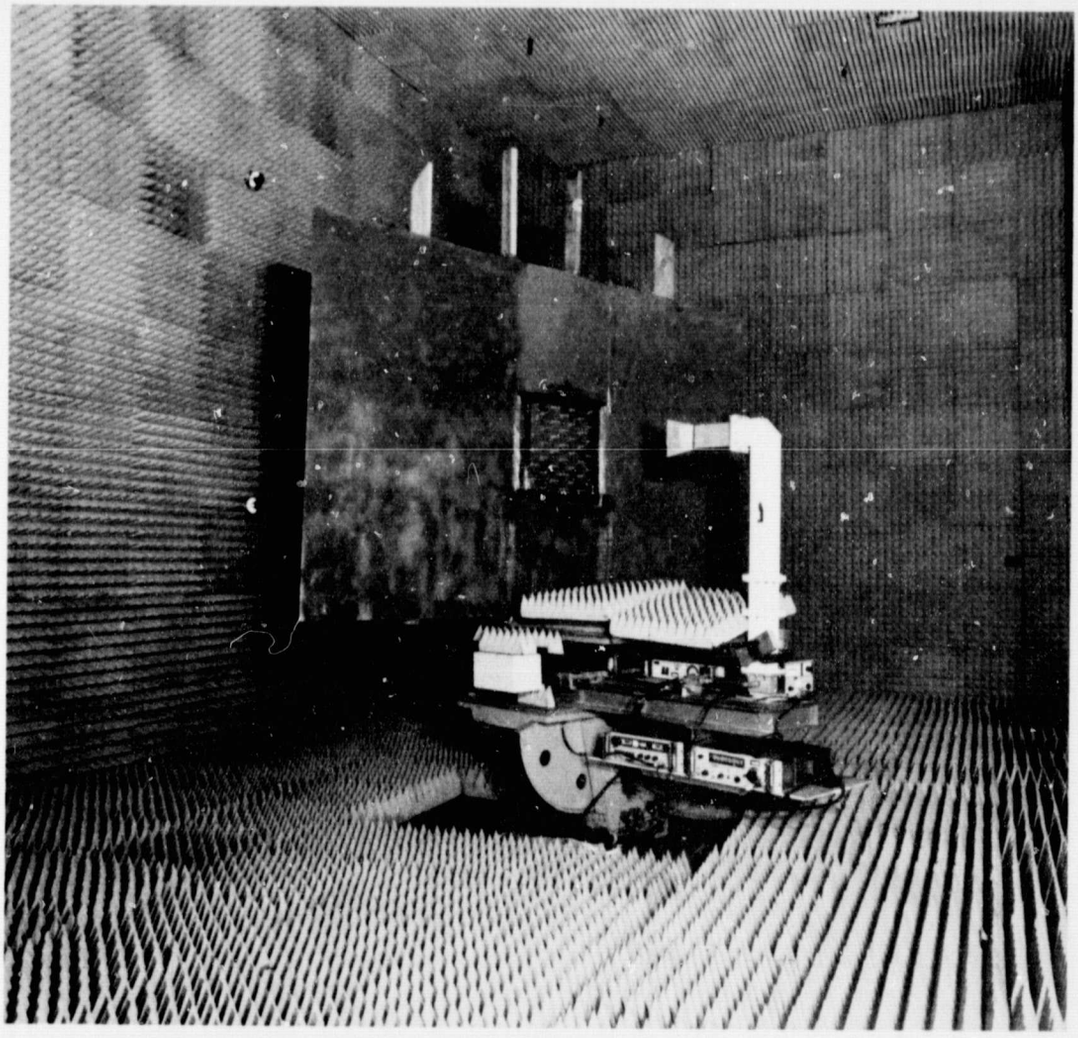

Figure 4-3. Rectenna Subarray in Ground Plane Fixture

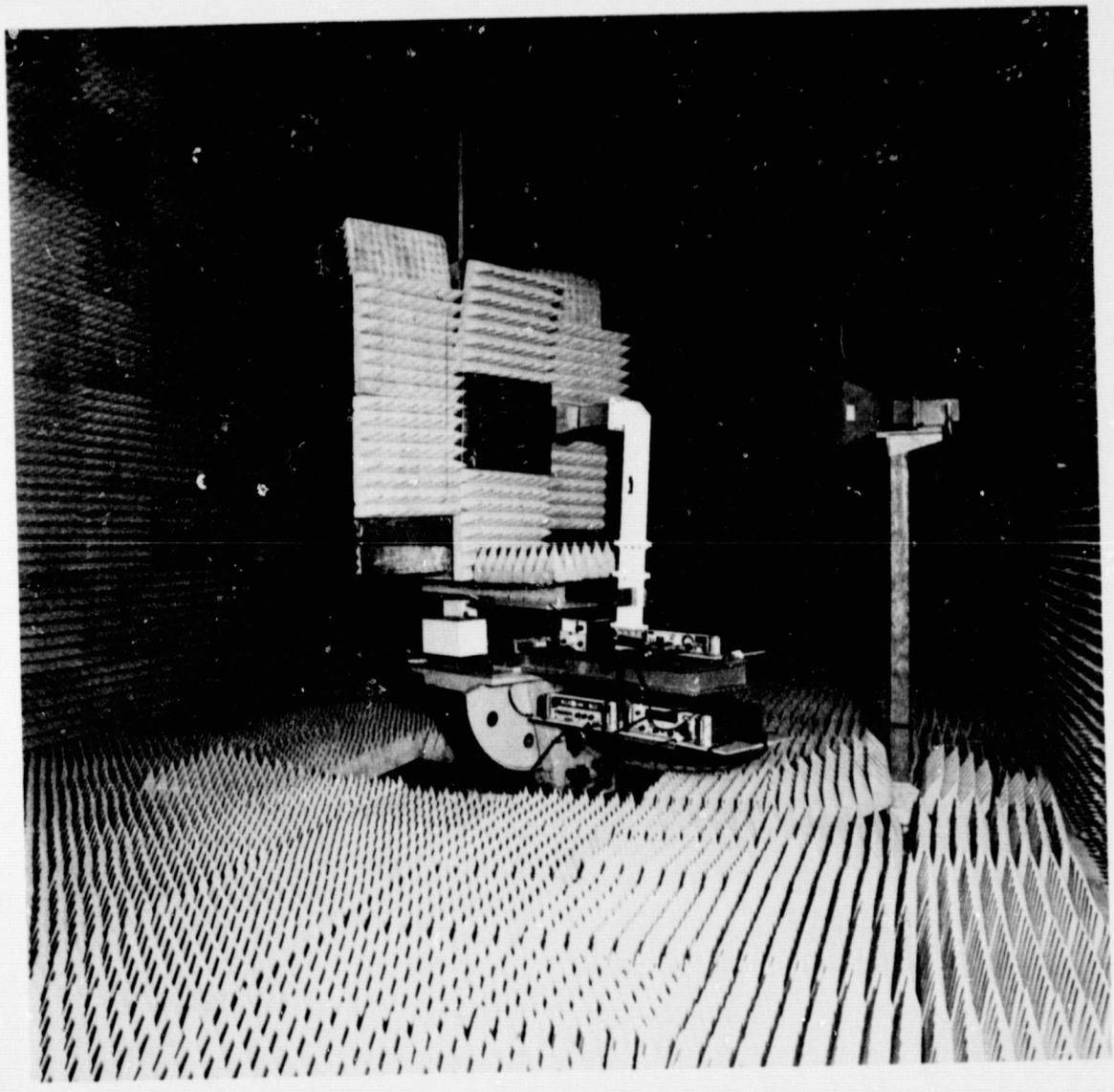

Figure 4-4. Rectenna Subarray in Absorber Fixture

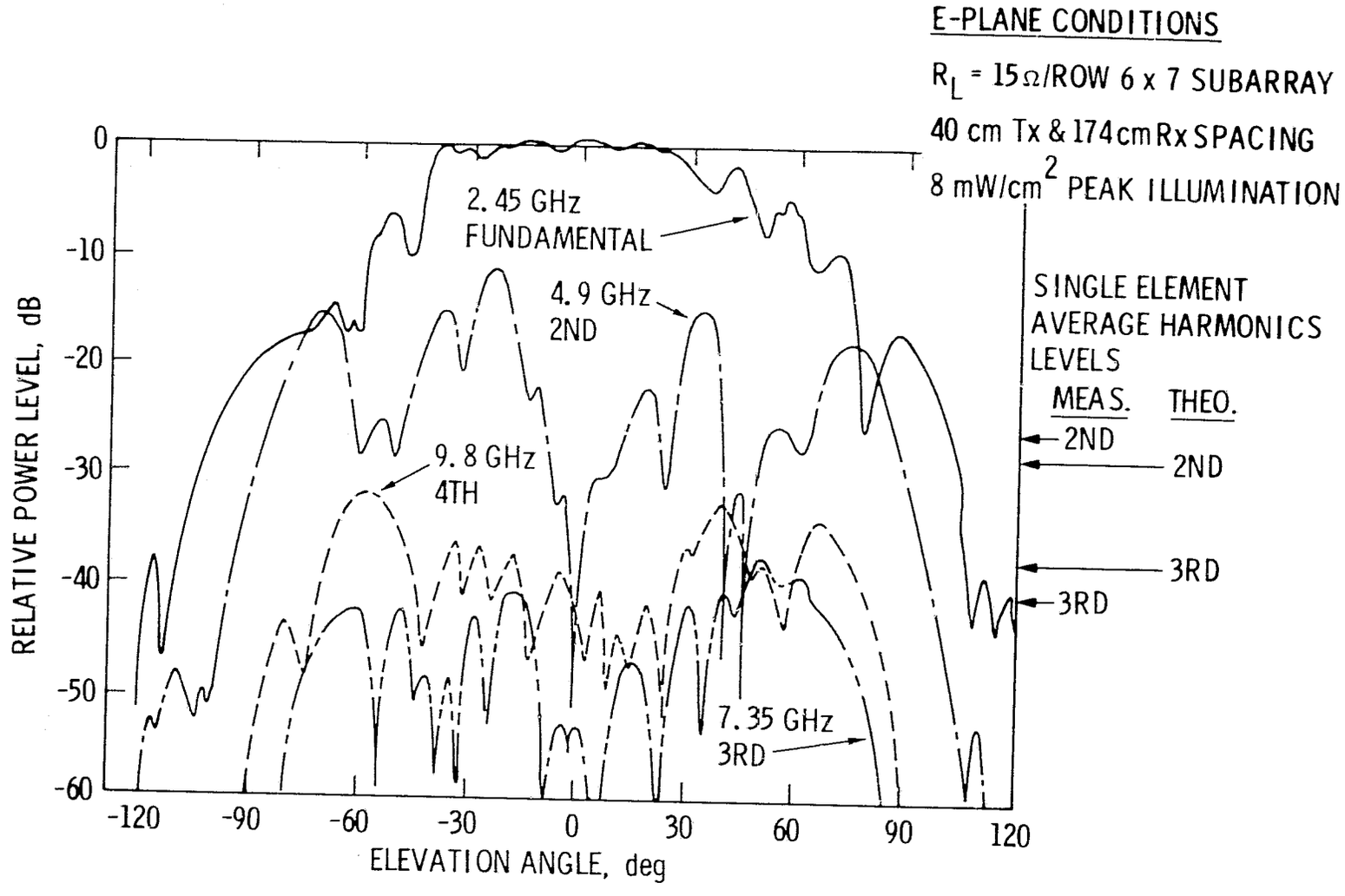

Figure 4-5. Resistively Loaded Rectenna Patterns

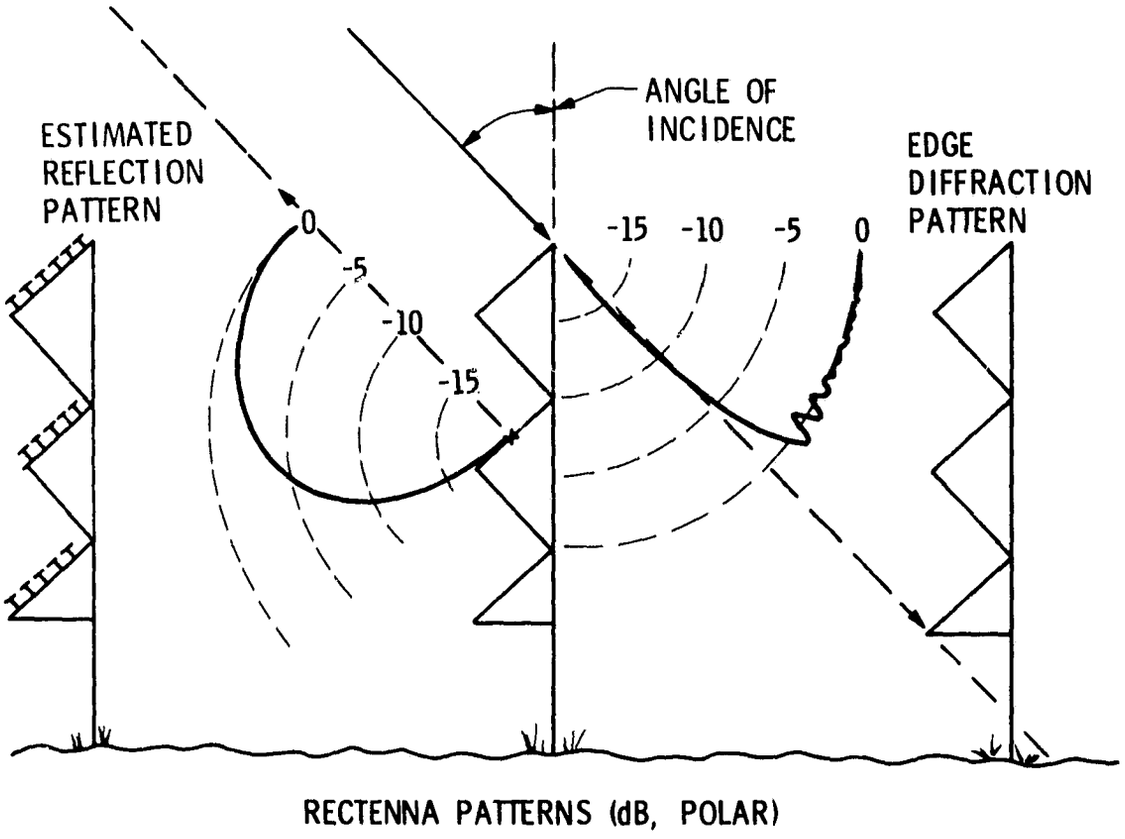

Figure 4-6. Rectenna Diffraction and Reflection Patterns

B. HARMONIC RERADIATION PATTERNS

1. General Discussion

The harmonic radiation of the rectenna is generated by the same rectifying diode that performs the conversion of the fundamental RF-to-dc output. The wave shapes of current required for efficient conversion are rich in harmonics (Reference 4-3). For efficient conversion the harmonic energy is generally trapped near the diode by the input and output low-pass filters at both the RF input and the dc output. However, a small but finite value of the harmonic energy is reradiated. Because the dipoles are longer than a half wavelength at the harmonic frequencies, are spaced above the ground plane by more than a quarter wavelength, and in their subarray positions are additionally separated by more than a wavelength, the resulting pattern of harmonic radiation is quite complex, with multiple grating lobes and peak levels at other than broadside positions in space about the subarray. The effective radiating impedance of the rectenna dipole element with diode generator is not known.

Because of these factors, the experimental approach described in the Appendix was undertaken to permit characterizing the harmonic radiation amplitudes and patterns of a rectenna subarray.

2. Measured Patterns

Figures 4-2 and 4-5 show the harmonics up to the fourth for a short-circuited rectenna and a resistively loaded rectenna respectively. The subarray elements have three section RF filters in balanced transmission line form. Figure 4-5 has annotations for the theoretically (Reference 4-3) calculated and individually measured (in a special test fixture, Reference 4-4) element harmonic total levels that may be compared to the recorded patterns levels. The peak radiated harmonic levels are higher than the predicted total average harmonic levels. The odd harmonics have a null on axis as expected from the balance fed, balanced dipole radiating element. The fourth harmonic radiation level is higher than the third, however.

At low levels of intensity of illumination, the second harmonic pattern and its amplitude relative to the fundamental frequency reflected signal stay essentially constant over a wide range of input power variations, and for various angles of incidence of the illuminator. Details are discussed in the Appendix.

For a large array of rectenna subarrays, the harmonic patterns are expected to be similar in angular distribution because of the effective phase random variations from each subarray. Therefore, the power will add randomly instead of coherently at a particular direction in the far field from a collection of rectenna subarrays.

Because of the triangular spacing of the rectenna dipoles, the grating lobe locations are not coincident with the E-plane pattern cuts. It appears from Figures 4-2 and 4-5, that the second harmonics radiation peaks are not exactly at the predicted grating lobe positions, and that the higher harmonic patterns are so complex that it is even more difficult to state with precision that the harmonic patterns are merely randomly phased grating lobe patterns. Significant radiations at the higher harmonics are expected from the exposed filter elements, in addition to the dipole wings, for the configuration. A new design by W. C. Brown encases the filters in a metallic environmental cover that should permit harmonic radiation only from the dipole antenna arms. An exception could be harmonic radiation of the "rusty bolt" variety, wherein a mechanically loose connection produces harmonics when vibrated while being RF illuminated.

C. BANDWIDTH

1. Rectenna Discussion

The bandwidths of the rectenna and slotted waveguide antennas are of interest in regard to the degree of discrimination that may be provided to spurious signals around the desired RF carrier, or in regard to the width of the low-loss region immediately around the carrier that may be employed to spread the carrier so as to reduce the average power flux density in any particular 4 kHz band.

2. Rectenna Measurements

Figure 4-7 shows the measured bandwidth with reference to the dc power output from the rectenna model employed for the scattered and harmonic pattern measurements. The close-spaced illuminator condition produces a higher total power output, but the taper of the illumination across the rectenna subarray is severe. The peaked output condition resulted in a more narrow bandwidth at the -1 dB level as compared to the lower level, but a more uniform illumination condition for the more distant input horn illuminated condition.

It would appear that it may not be difficult to achieve a rectenna design that could cover the entire ISM band without significant loss. The rectenna elements in this test were originally tuned for peak performance at a frequency of 2.388 GHz for the Goldstone tests in 1975. There is some detuning with power level variation, which would be expected because the diode effective capacitance changes with bias level. The scatter in the measured data points is due to internal resonance modes set up within the large metal box that forms the enclosure for the rectenna buss bars, behind the ground plane of the dipoles. Unbalanced currents leak off the balanced transmission lines that project through the ground plane.

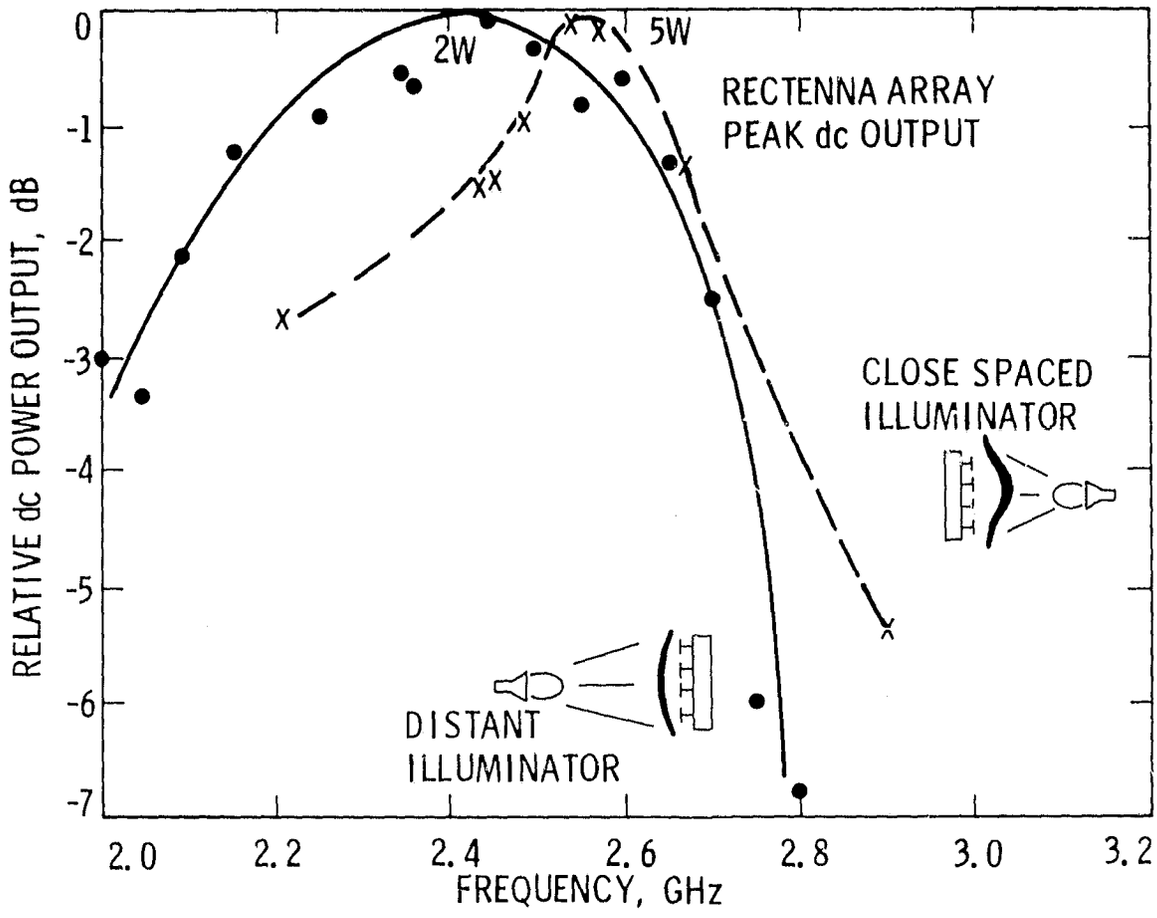

Figure 4-7. Rectenna Bandwidth

3. Slotted Waveguide Discussion

The bandwidth of the slotted waveguide radiating antenna is expected to be much narrower because of the nature of the resonant standing wave array. Typically, the bandwidth is characterized as proportional to 1/n, where n is the number of slots.

4. Waveguide Measurements

Figure 4-8 shows the measured impedance bandwidth of several slotted waveguide radiators produced by JPL, Boeing, and Raytheon in connection with Beamed Power Technology and SPS investigations. The 1.5:1 VSWR bandwidth ranges from a minimum of $\pm 0.4\%$ to $\pm 2\%$ for the 64-slot array, depending upon the tuning pattern of the input waveguide. The ISM band is $\pm 2\%$ in S-band; thus, a wideband standing wave slotted waveguide radiator subarray would be limited to a very small number of slots. Conversely, the narrow bandwidth may be of advantage in providing extra filtering of spurious signals near the power carrier for the case of a large number of slots, in a high-gain subarray. However, the operating environment and construction tolerances will tend to limit the predictable center frequency and bandwidth for very narrow band subarrays.

D. RECTENNA NOISE

1. General Discussion

In addition to the straightforward reflection of a portion of the fundamental frequency signal from a rectenna, there is expected to be an emitted noise component around the carrier, even if none were originally present. This noise component is added by the diode rectification process. This plasma noise is similar to space charge spectrum spreading and shot noise, that is, incidental modulation produced by the klystron or solid-state dc-to-RF converter spectrum. Because the noise spectrum is centered around the incoming carrier frequency, it will readily pass through the input low-pass filter and will be radiated efficiently by the rectenna dipole.

2. Measurements

A crude measurement of the noise level was attempted around the reflected fundamental at 50 MHz spacing from the carrier (at 2.45 GHz), and in the 10 MHz bandwidth of a spectrum analyzer with about -80 dBm threshold detectability response. The rectenna was grossly underexcited, due to equipment limitations at the time, with only +30 dBm illumination from a small horn and with a high impedance load of 1 kΩ across 6 paralleled elements in each row. Six volts of dc was produced in the central row, however, indicating that the diodes were conducting.

From the negative results, all we can say is that the reflected fundamental noise for these conditions was less than -80 dBm in a 10 kHz bandwidth at 50 MHz from the carrier. The noise level in a 4 kHz

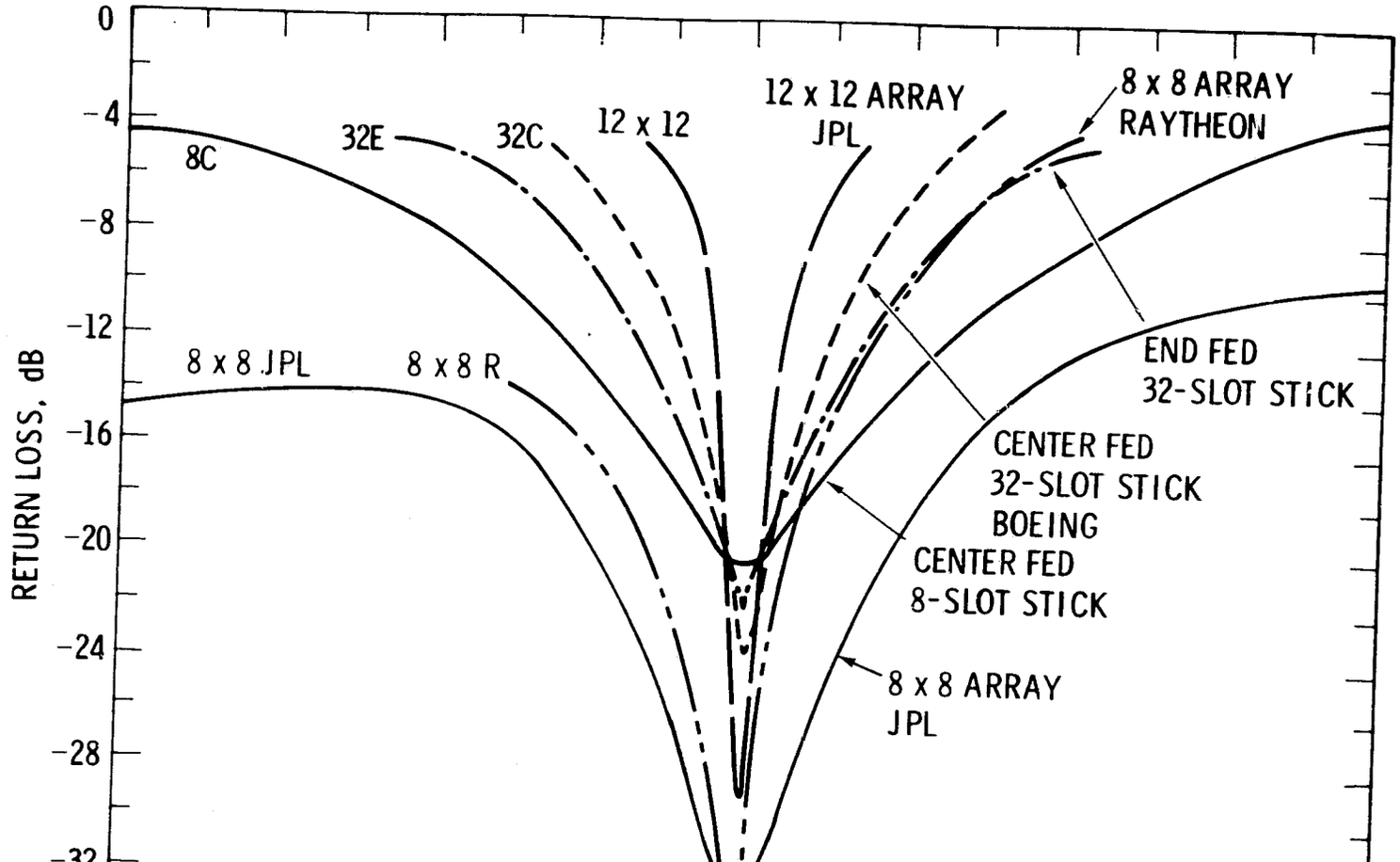

Figure 4-8. Impedance Bandwidth of Slotted Waveguide Radiators

bandwidth is expected to be similar to that of the dc-to-RF converters. A similar low-level sideband of noisy character radiation is expected around the harmonic frequencies also. The harmonic noise levels were not measured in this effort.

SECTION V

CONCLUSIONS

The electronic equipment at either end of a microwave beamed power transmitting link radiates undesired RF energy as a byproduct of performing its design function. The levels and directions of this energy are a function of the initial design of the equipment, the operating conditions and environment, and the state of maintenance. After the initial installation, some added filtering or variation in operating parameters may reduce the level or change the direction or polarization of the undesired radiation, but the best course of attack to minimize the undesired radiation is to provide, at the outset, converters of clean design, along with high signal-to-noise ratio (SNR) drive signals. The entire chain of RF frequency generation of reference or pilot signals, their transmission, propagation, reception, phase reference origination and distribution, phase comparison and conjugation, phase control and high-power amplification, radiated signal comparison, propagation over the return path, reception collection, and, finally, rectification, must be thoroughly modeled, analyzed, and engineered, in order to meet the required radio regulations.

Competing requirements will call for a design that can be economically fabricated, constructed, and maintained for the desired operating lifetime.

Techniques exist in the collection of microwave arts that may be applied to reducing the undesired radiations. The selection of certain configurations of microwave structure over others, for example, may yield lower scattering or phase errors, or yield lower current conduction loss, or provide lower intermodulation product (IMP) conversion. Filtering can be applied to signals before they are radiated and after they are received. Natural structure shielding or filtering can be used to advantage, and even the electronic structure or spectrum of the RF signals can be shaped or engineered to assist in minimizing a particular interference design problem. Particularly objectionable signals, such as certain harmonics that are specific in nature and not truly random, can be dealt with by techniques of balancing or bucking out, which are active in nature instead of simply passive as in conventional filters. However, a price must be paid in terms of complexity and reliability of the resulting system. Nevertheless, the total life-cycle cost tradeoff may be worthwhile in terms of yielding an environmentally acceptable performance while satisfying the main design objective of transmitting energy without wires. Frequency allocations are difficult to obtain and are not easily changed. The ISM band frequencies are not integrally related, and thus the beamed power transmission link designer must be prepared to cope with the design of filtering schemes to greatly reduce the harmonics attendant on generating high-power microwaves. Spectrum processing techniques such as frequency modulating or dithering the power carrier within the available band (Reference 5-1) may assist in reducing the average spectral power density in specific bands of frequencies. Polarization modulation may also be appropriate in some circumstances.

Maintenance of the original design physical condition will be necessary to assure continued acceptable performance. Also, the operating parameters must be confined within a predetermined range. Out-of-tolerance conditions must be corrected and failed elements must be replaced or repaired.

SECTION VI

RECOMMENDATIONS

Additional and more accurate measurements of parameters and performance must be conducted under better simulated conditions and environments in order to provide more detailed definition of Beamed Power Transmission System performance. The preliminary data in this report will permit better initial definition of system RFI characteristics, but the additional data taken under more nearly true operating conditions, when coupled with refined modeling and analysis methods, will extend the evaluation to larger and improved design hardware.

Instrumentation and measuring equipment that can handle high power and that possess valid characteristics at all the harmonics in question are sorely needed. Techniques for making more accurate measurements of the noise level close to the carrier, and also of the harmonics, are required to better determine the converter spectrum.

In order to increase the accuracy of predicting harmonic radiation pattern levels, it will be necessary to develop and test modeling and analysis techniques for harmonic generation in converters, including the impedances presented at the harmonic frequencies. It will also be necessary to predict the transfer characteristics of multimode propagation, and develop analytic models of the elemental radiators at the harmonics.

The effects of propagation conditions on the performance of a Beamed Power System need to be analyzed not only to determine the loss of power transferred under nonstandard conditions, but also to determine the resulting distribution of the scattered energy. Those applications requiring dynamic beam positioning will be very difficult to encompass with modeling that accounts for all the transmitted and scattered energy. It should, however, be attempted.

Special shaping of the radiated power spectrum should be investigated to minimize interference effects. Frequency modulation of the carrier or other frequency deviation patterns may be able to decrease the average power flux density in particular channels. The effect on the harmonics should be evaluated also, as the results there may also be beneficial; on the other hand, they may render matters worse, depending upon circumstances in the harmonic bands.

The harmonics should be subject to definitive engineering control, since they are generated at precisely known frequencies. A scheme for bucking out the major magnitude of the harmonics with a precisely controlled antiphase signal of the proper magnitude at each discrete harmonic would appear to be possible in principle. The cost of automatic monitoring and control circuitry to maintain minimum acceptable harmonic generation levels may be high, in practice, but in terms of permission to operate, affordable to the system.

Different rectenna configurations that possess poor radiating characteristics at the harmonic frequencies should be investigated. Configurations that provide natural shielding for harmonics may be also attractive. Designs for control of operating parameters such as ground plane spacing, load value management, operating frequency, polarization, or incident flux density may be necessary to adequately control the level of reflected fundamental signal at the rectenna.

Pattern measurements that are keyed to looking for cases of harmonic focusing that could accompany the electronic beam steering at the fundamental frequency need to be conducted. If there are inherent correlated processes at the harmonic frequencies in the active retrodirective array phase control process, then there may be significant focused lobes at the harmonics.

The application of beamed RF power is technically feasible, although system economics, including the cost of safety, affects the practicality of the concept. The technical performance, however, is satisfactory in terms of actual power generation, transmission, reception, and reconversion efficiencies and power levels. A modest demonstration could provide the focus for detailed system and individual component design to meet the existing radio regulations and thereby provide a better measure of the regulations' affects upon the system performance.

REFERENCES

1-1. Dickinson, R., and Brown, W., Radiated Microwave Power Transmission System Efficiency Measurements, Technical Memorandum 33-727, Jet Propulsion Laboratory, Pasadena, Calif., May 15, 1975.

1-2. Dickinson, R., Evaluation of a Microwave High-Power Reception-Conversion Array for Wireless Power Transmission, Technical Memorandum 33-741, Jet Propulsion Laboratory, Pasadena, Calif., Sept. 1, 1975.

1-3. Brown, W., "Optimization of the Efficiency and Other Properties of the Rectenna Element," 1976 IEEE MTT-S International Microwave Symposium Digest of Technical Papers, pp. 142-144.

1-4. Lien, E., "High Efficiency Klystron Amplifiers," MOGA Conference Proceedings, pp. 11-21 to 11-27, Sept. 1970.

1-5. Edition of 1976 Radio Regulations Published by the General Secretariat of the International Telecommunications Union, Geneva, 1976.

1-6. Foster, C. F. "Automated Fourth-Harmonic Analyzer," DSN Progress Report 42-37, Jet Propulsion Laboratory, pp. 105-111, Nov. and Dec. 1976, 15 Feb. 1977.

1-7. Staprans, A., et al., "High-Power Linear-Beam Tubes," Proceedings of the IEEE, Vol. 61, No. 3, pp. 299-330, Mar. 1973.

1-8. Kosmahl, H. G., and Albers, L., "Three-Dimensional Evaluation of Energy Extraction in Output Cavities of Klystron Amplifiers," IEEE Transactions on Electron Devices, Vol. Ed-20, No. 10, pp 883-890, Oct. 1973.

1-9. Cown, B., et al., "Statistical Prediction Model for EMC Analysis of Out-of-Band Phased Array Antennas," IEEE Transactions on Electromagnetic Compatibility, Vol. EMC-18, No. 4, pp. 163-170, Nov. 1976.

1-10. Ormsby, J., "Antenna, Load, and Field Effects on the Bistatic Scattering Patterns from a Linear Dipole Array," IEEE Transactions on Antennas and Propagation, Communications, Vol. AP-27, No. 1, pp. 116-122, Jan. 1979.

2-1. Barnes, J. et al., "Characterization of Frequency Stability," IEEE Transactions on Instrumentation and Measurements, Vol. IM-20, pp. 105-120, May 1971.

2-2. Finnegan, E., "Measurement of Klystron Phase Modulation Due to AC-Powered Filaments," DSN Progress Report 42-40, Jet Propulsion Laboratory, pp. 152-155, May and June 1977.

2-3. Kerr, D., Propagation of Short Radio Waves, McGraw-Hill Book Co. Inc., N.Y., N.Y., 1951.

2-4. Mohr, H., "A Reactive Fourth-Harmonic Filter Operating at 400-kW CW," IEEE Transactions on Microwave Theory and Techniques, Vol. MTT-26, No. 5, pp. 341-345, May 1978.

2-5. Bathker, D., et al., Single- and Dual-Carrier Microwave Noise Abatement in the Deep Space Network, Technical Memorandum 33-733, Jet Propulsion Laboratory, Pasadena, Calif., Aug. 1, 1975.

2-6. Woo, R., and Ishimaru, A., "A Similarity Principle for Multipacting Discharges," Journal of Applied Physics, Vol. 38, No. 13, pp. 5240-5244, Dec. 1967.

2-7. Satellite Power System, DOE/ER-0034, Concept Development and Evaluation Program, Reference System Report, US Department of Energy and The National Aeronautics and Space Administration, Oct. 1978.

4-1. Kraus, J., Antennas, McGraw-Hill Book Co. Inc., N.Y., N.Y., p. 47, 1950.

4-2. Stark, L., "Radiation Impedance of a Dipole in an Infinite Planar Phased Array," Significant Phased Array Papers, R. C. Hansen, Editor, Artech House, Inc. Dedham, Mass., pp. 94-103, 1973.

4-3. Nahas, J., "Modeling and Computer Simulation of a Microwave-to-DC Energy Conversion Element," IEEE Transaction on Microwave Theory and Techniques, Vol. MTT-23, No. 12, pp. 1030-1035, Dec. 1975.

4-4. Brown, W. Electronic and Mechanical Improvement of the Receiving Terminal of a Free-Space Microwave Power Transmission System, NASA CR-135194, PT-4964 for NASA Lewis Research Center Contract NAS 3-19722, p. 61, Aug. 1977.

5-1. Report No. 679, "Characteristics and Effects of Radio Techniques for the Transmission of Energy From Space," International Telecommunication Union, International Radio Consultative Committee, Recommendations and Reports of the CCIR, 1978, XIVth Plenary Assembly Kyoto, 1978, Vol II. Space Research and Radioastronomy, Geneva 1978.

APPENDIX A

PATTERN MEASUREMENT SYSTEMS

The description of the equipment setup and instrumentation, along with the techniques employed for recording the harmonic patterns of the slotted waveguide rediators and the rectenna subarray, will be presented in this section.

A. SLOTTED WAVEGUIDE HARMONIC PATTERN MEASUREMENTS

The harmonic patterns were measured of the 64-element subarray antenna, an 8-slot waveguide stick, and an abrupt coax-to-waveguide transition. The amplitudes of the received harmonics were calibrated at the harmonic frequencies with the standard gain horn antennas shown in Figure A-1. The fourth and fifth harmonics could both be received by the smallest horn without ambiguity.

The measurement system block diagram is shown in Figure A-2. The pattern receiver's IF gain and pattern level controls were employed to set the recorded harmonic pattern level to the absolute chart pen position which was the same as the fundamental frequency. This position was at the largest amplitude grating lobe levels near the axis of the antenna under test, corresponding to the gain at the peak of the beam of the fundamental frequency of the antenna. By keeping track of the illuminating horn gain, the RF generator output power, the recorder gain settings, and the ranges at the various frequencies, it was possible to solve for the harmonic peak gain level with respect to the fundamental frequency pattern peak gain level.

Samples of the transmitted power were monitored near the TWTA outputs during the test pattern recordings in order to verify that the illuminating power did not vary more than ±0.2 dB, and to monitor the precise harmonic frequencies from the signal generator.

The dimensions of the radiating slots as measured in wavelengths at the harmonic frequencies, particularly the fifth, are large and could support crosspolarized radiation in addition to the normally polarized emissions. Therefore, it was necessary to search polarization as well as azimuth or elevation around the antennas in order to seek out the highest levels of harmonic emission.

Pattern cuts were made in the E, H, XE, and XH planes. E-plane cuts refer to a rotation of the antenna under test in azimuth, such that the normal excitation at the fundamental frequency causes the electric field vector across the narrow dimension of the slot in the radiating waveguide to lie in the plane of rotation. The H-plane pattern cut is obtained by positioning both the test and illuminating antennas such that they are orthogonal in position about the beam axis to that of the E-plane cuts. The XE and XH cuts refer to patterns recorded with the illuminating antennas polarization positioned orthogonal to what it would be for a normal E- or H-plane cut, respectively.

The estimated accuracy of the recorded harmonic patterns is ±0.2 dB for the peak gain of the antenna at the fundamental and an additional

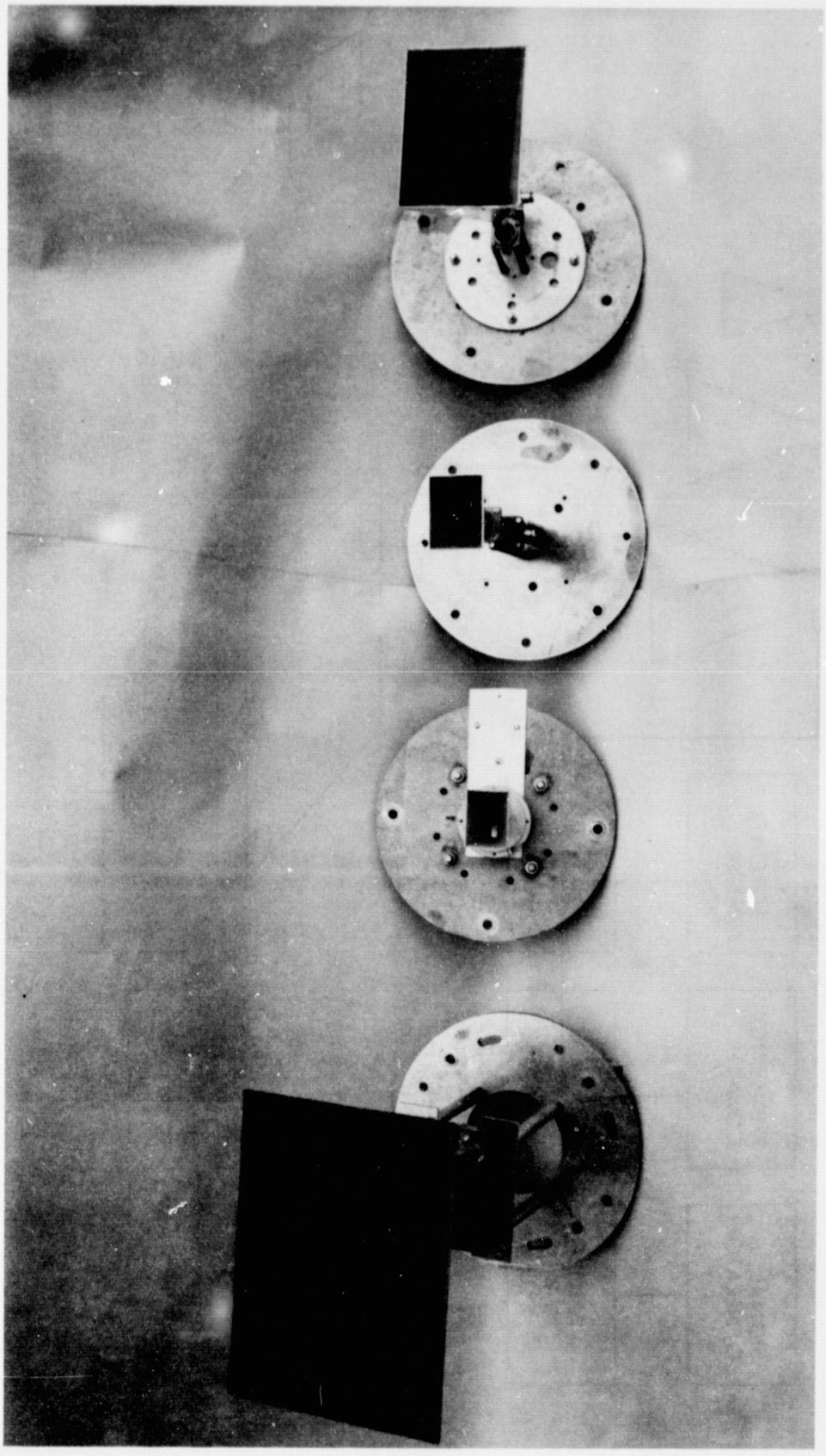

Figure A-1. S, X and K-Band Standard Gain Horns

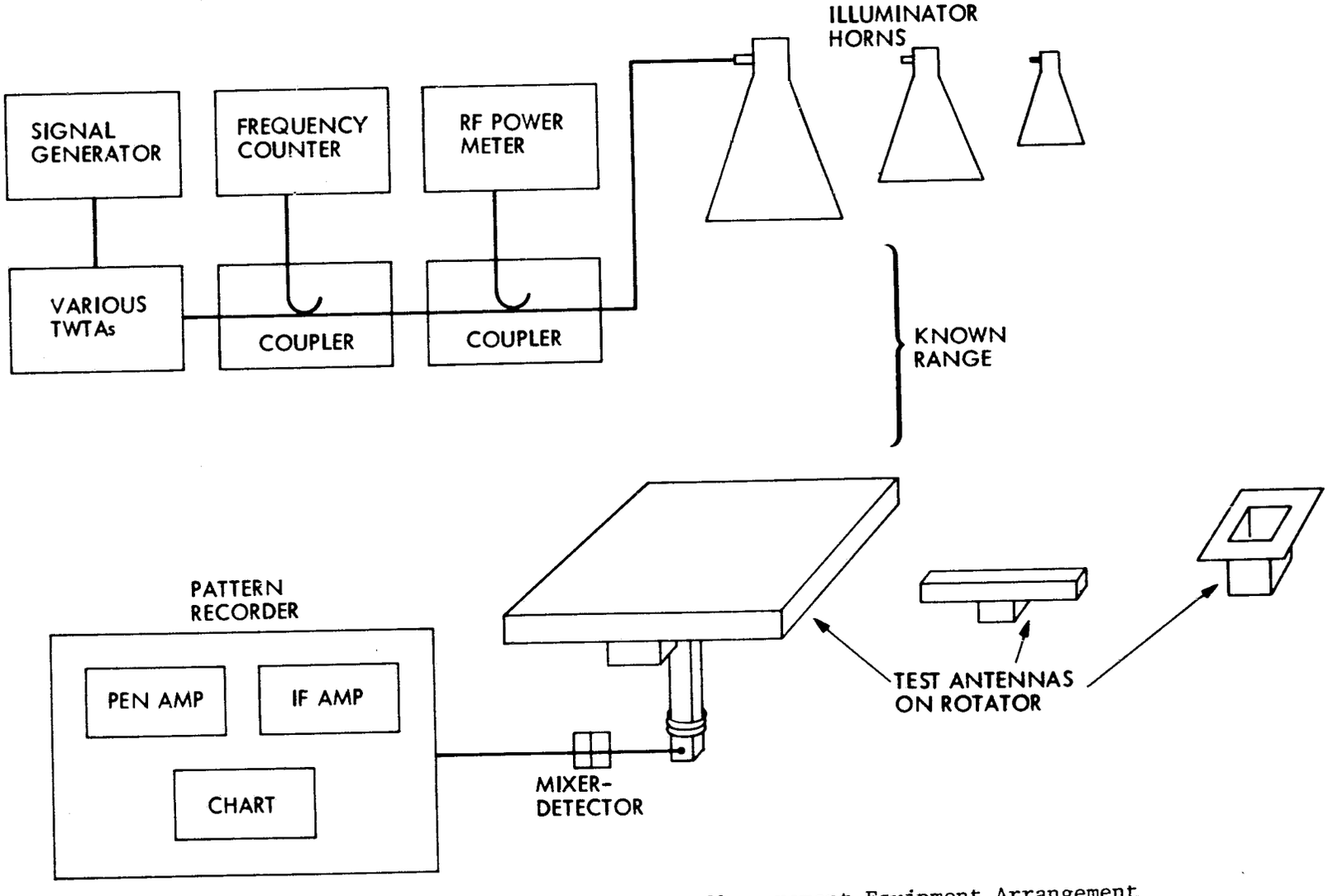

Figure A-2. Slotted Waveguide Antenna Measurement Equipment Arrangement

±0.5 dB per 10 dB below the peak. The second harmonic peak level with respect to the fundamental is estimated to be ±0.75 dB with the remainder of the pattern at ±1.5 dB per 10 dB below the peak. The accuracy deteriorates with the higher harmonics, where at the fifth harmonic it is estimated that the accuracy is only ±3 dB for the peak relative to the fundamental, and the remainder of the pattern is about an additional ±3 dB per 10 dB.

To insure that the harmonic radiation was coming from the antenna and not from a broken cable or loose connector, a "no-pattern" check with a termination in the receiver line was run at each harmonic test setup.

An additional potential source of error in the recorded harmonic patterns could be due to any large phase correlated areas on the surface of the antenna, because the patterns were recorded at a range of around 4 meters, which would be in the near field in that case. However, no identifiable main beam appeared in any of the harmonic patterns, thus indicating random phasing of the harmonic emissions.

The dimensions of the slotted waveguide subarray are given in Figure 3-2 and Table A-1.

Figure A-3 shows the 8-element waveguide stick, whose measured fundamental and harmonic patterns are shown in Figure A-4 (E-plane) and A-5 (H-plane). The stick is the model for the feed guide of the 8-stick subarray. The radiating patterns were made using the dismounted radiating slot faceplate shown in Figure A-3.

Figure A-6 shows the calculated, theoretical, fundamental, and harmonic patterns (by Michel E. Schwartz) in the H-plane of an 8-slot waveguide if all slots were fed in phase and supplied with equal power. Because of the random phasing due to multimode propagation in the real antennas, the actual patterns as indicated in Figure A-5 are much lower in gain and much more random in character.

B. RECTENNA SCATTERED AND HARMONIC PATTERN MEASUREMENTS

The rectenna subarray employed for recording the scattered fundamental frequency energy and the emitted harmonics is shown in the bistatic test setup in Figure A-7. The subarray consists of 7 rows of 6 rectenna elements each, arranged in a triangular lattice. Each row has a common buss bar for collecting the dc output from the rectennas. The individual elements are half-wave dipoles spaced 0.2 wavelengths from a solid aluminum sheet ground plane.

The low-pass filter assemblies of the rectennas project through the ground plane to the rectifiers and the buss bar. The subarray model was designed for wind tunnel tests during the development of the rectennas for the Goldstone tests in 1975. The elements are capable of handling 6 W of RF power each, at 2.388 GHz. The array is approximately 50 cm square.

Table A-1. 8-Stick Slotted Waveguide Subarray Dimensions (Refer to Figure 3-2) (F = Feed, R = Radiator)

Element	Dimensions cm	Dimensions (in.)	
a_R =	8.255	3.250	
a_F =	7.899	3.110	
b_R =	3.721	1.465	
b_F =	3.721	1.465	
C_R =	4.592	1.808	
C_F =	8.743	3.442	Straight, Not Folded
d =	0.871	0.343	
ℓ_R =	5.791	2.280	
ℓ_F =	5.969	2.35	
S_R =	9.147	3.601	
S_F =	9.804	3.860	
W =	0.470	0.185	
t_F =	0.051	0.020	
t_B =	0.051	0.020	
t_W =	1.207	0.475	Gapped
θ =	15-1/2 deg		

Excluding the extended feed guide shorts, the radiating faceplate overall dimensions are 78.105 cm (30 3/4") E-plane by 75.565 cm (29 3/4") H-plane.

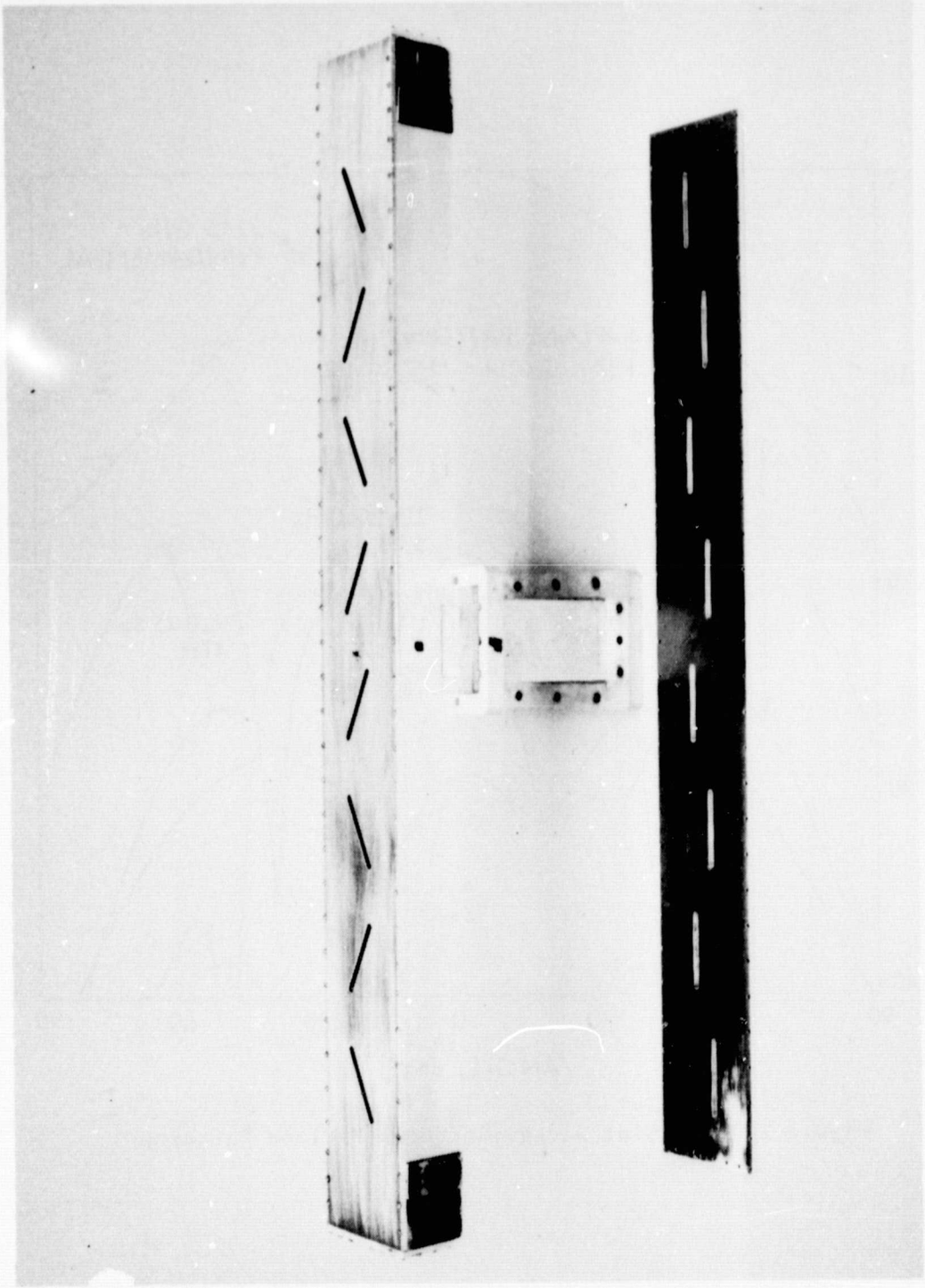

Figure A-3. 8-Element Waveguide Stick

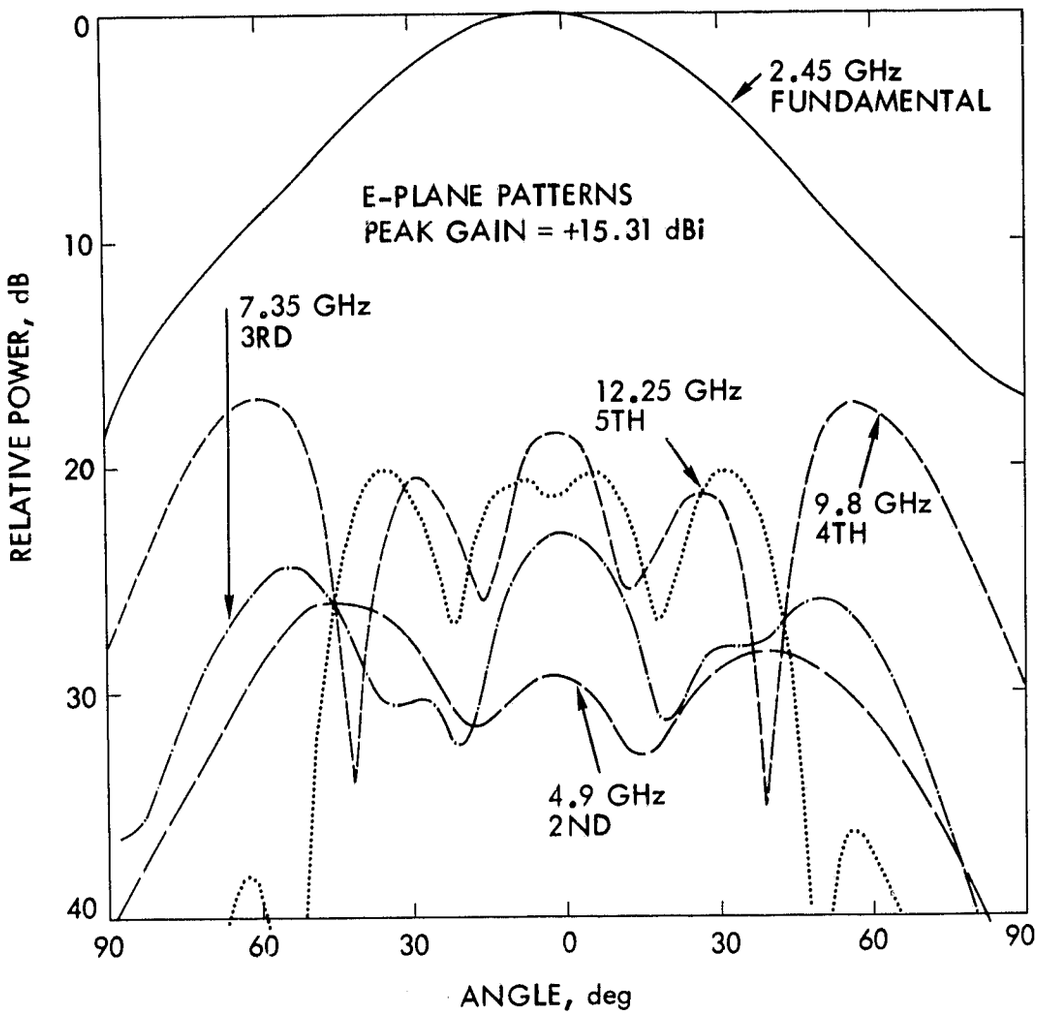

Figure A-4. 8-Slot Waveguide Stick E-Plane Patterns

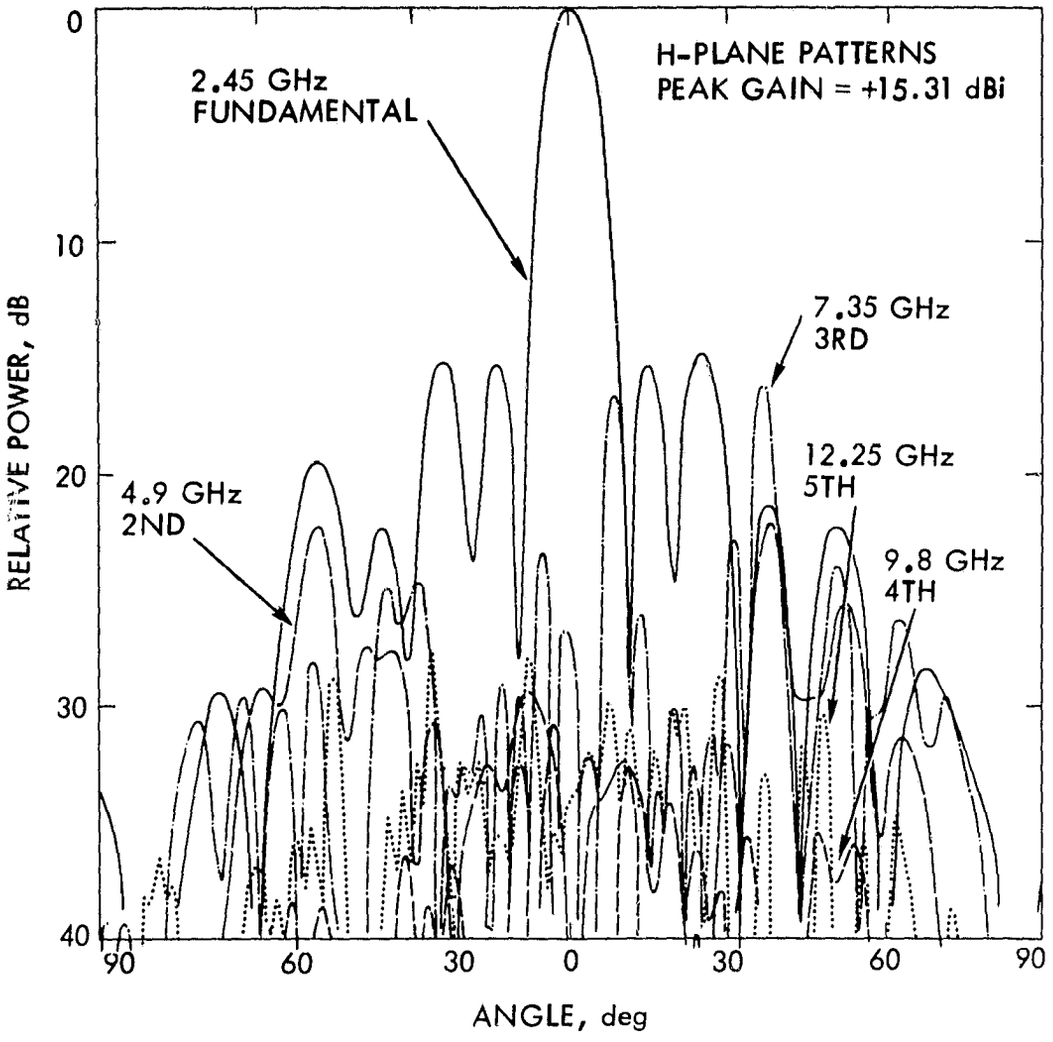

Figure A-5. 8-Slot Waveguide Stick H-Plane Patterns

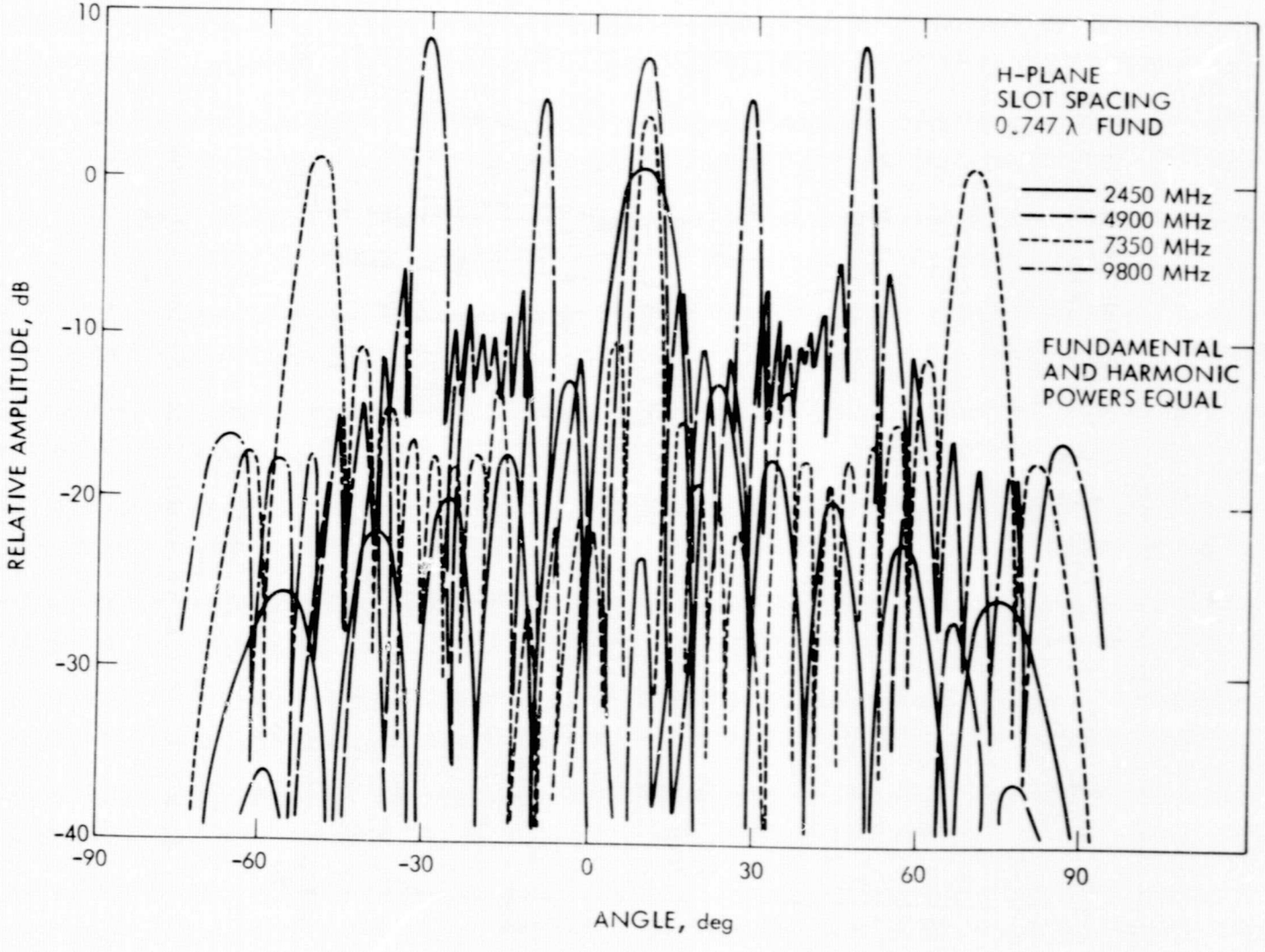

Figure A-6. Theoretical H-Plane Patterns of 8-Slot Waveguide

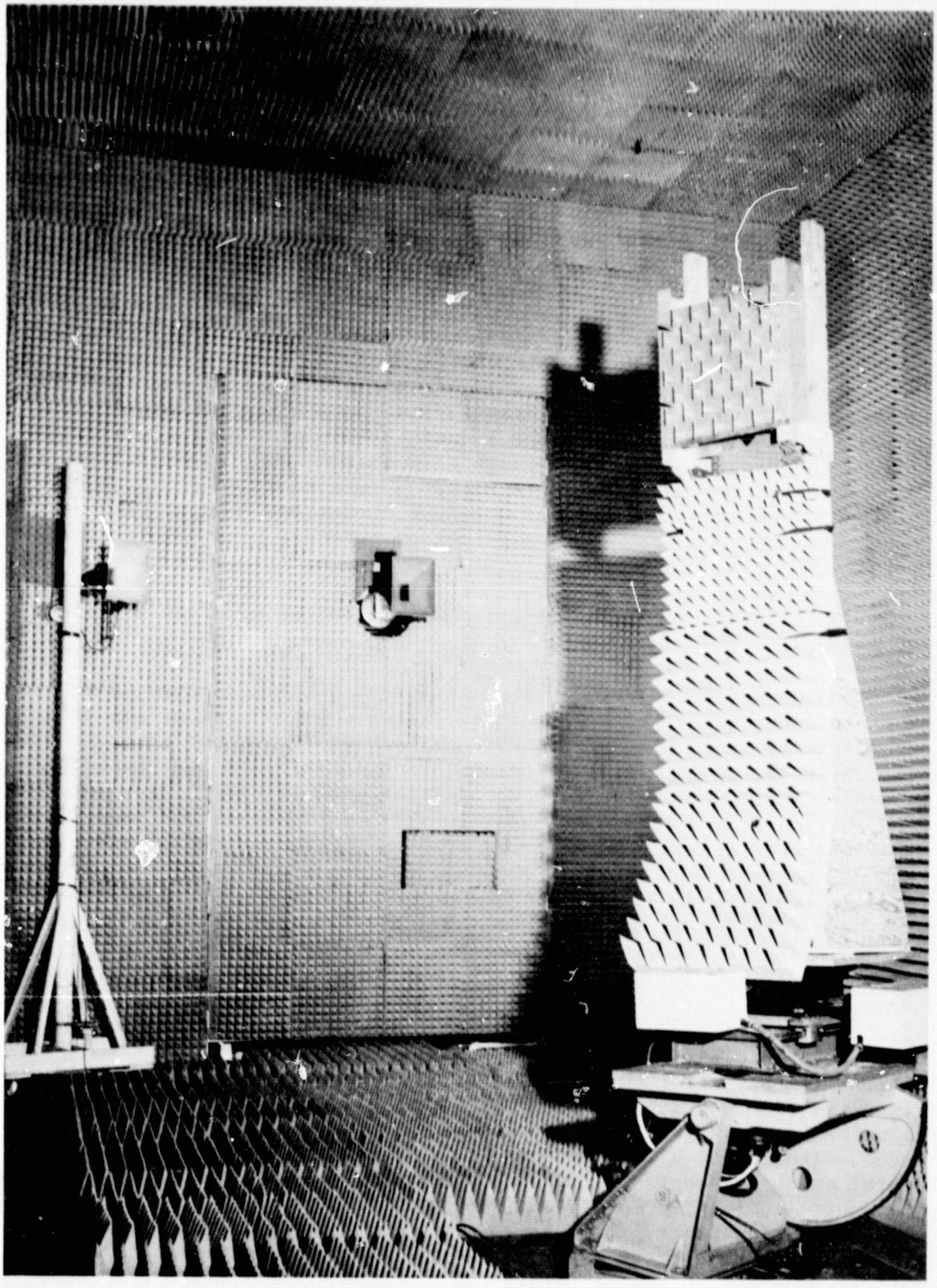

Figure A-7. Rectenna Bistatic Pattern Range Configuration

The bistatic tests were conducted as a precursor to check the pattern receiving system and mounting arrangement, and to document the low-level intensity illumination performance of a rectenna subarray. The pattern is shown in Figure A-8. By comparing the bistatic pattern level direct and cross-polarized, the effects of the rectenna element phase coherency can be estimated. That is, the reflected patterns would be identical if the dipoles and their impedances were all identical. The lower gain of the normally polarized signal is less than the cross-polarized signal, and reflects the random phasing scattering of the incident RF. For crossed polarized illumination, the rectenna dipoles are essentially transparent and the reflection pattern is that of the underlying ground plane.

The bulk of the reflected fundamental and harmonic patterns were recorded with the test setup shown in Figure A-9. Limited-output power-level generating equipment was available for illuminating the rectenna subarray. With only a 20 W TWTA available, the choice was either long range illumination spacing, with consequent low-level uniform illumination of the rectenna, or short range illumination spacing, resulting in high-level tapered illumination. Patterns were recorded for both spacing conditions and the receiving antennas at various ranges. The patterns were analyzed for any significant differences as a result of the two different illumination conditions. No great differences were noted. Figure A-10 shows the output dc power distributions under the different illumination conditions and for certain differences in dc load resistance magnitudes.

The patterns were recorded at different pick-up antenna ranges in order to look for any high-gain (i.e., large coherent reflection area or uniform coherent harmonic conditions) pattern characteristics. However, with the modest level of illumination, the diodes are turned on enough to result in sufficient phase differences to destroy any large contribution from a coherent high-gain region. That is, the individual diode's phases are random enough to destroy any common phase condition, such as occurred with the very low-level illumination condition encountered in the bistatic patterns. The degree of this decorrelation may well be a function of the absolute level of illumination, however, and one would expect the patterns to change as a function of the illumination.

The estimated combined collection and conversion efficiency of the subarray, the central row, and an individual element are compared to the large Goldstone array on the basis of operating conditions, as shown in Figure A-11. The wind tunnel model subarray is obviously under-illuminated. However, for the various conditions shown, we could not detect significant differences in the character of the reflected fundamental or the harmonics patterns. The relative levels compared to the incident illumination level, and the pattern shapes and distributions, were rather invariant. Thus the recorded patterns are felt to be representative of the rectenna array. Furthermore, the rectenna illuminating horn antenna has an approximately $\cos^6\theta$ pattern shape appropriate for the approximately 12 to 15 dB gain of a standard gain horn, whereas the reflected fundamental envelope pattern is commensurate with the broad

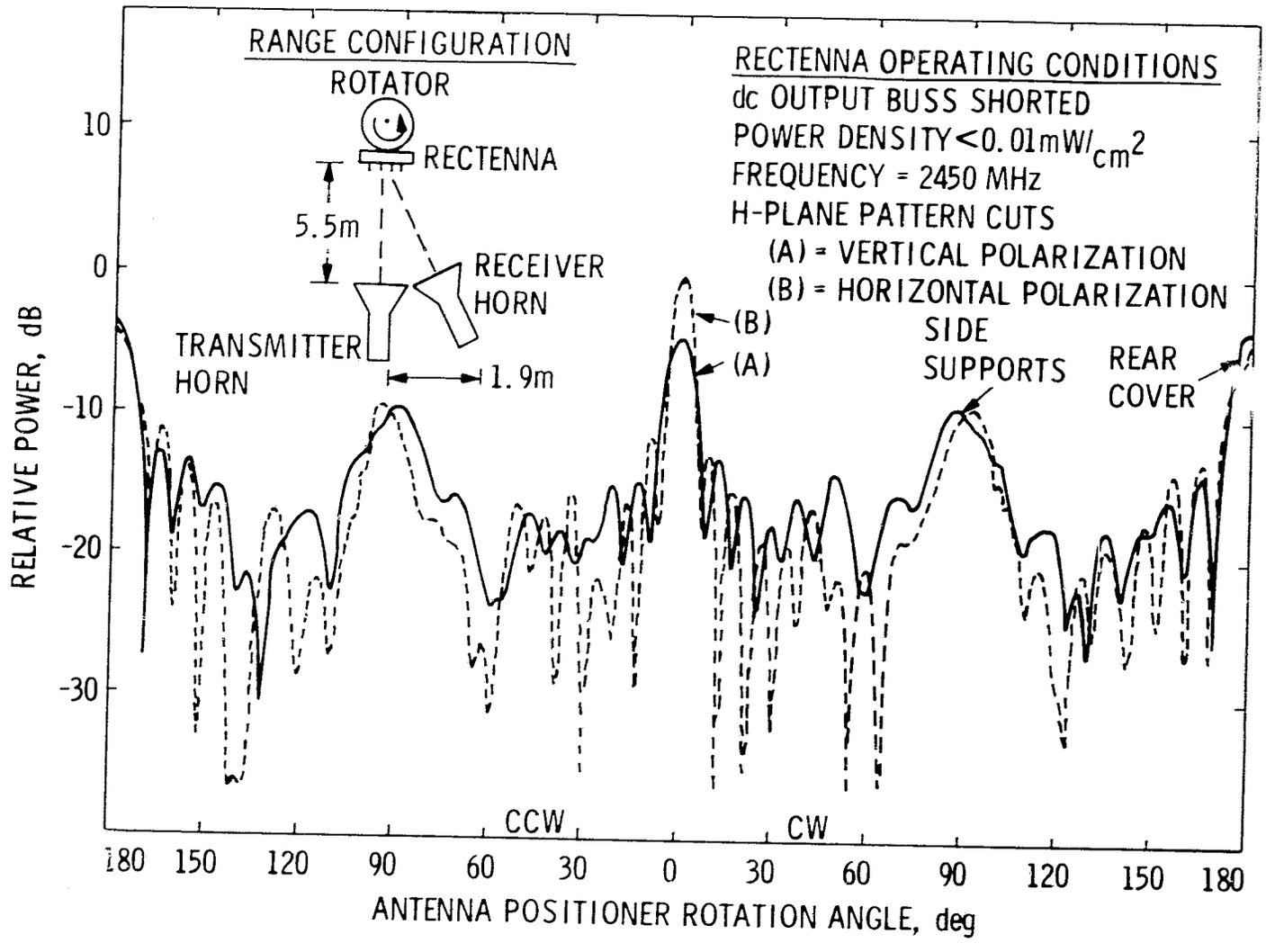

Figure A-8. Rectenna Bistatic Patterns

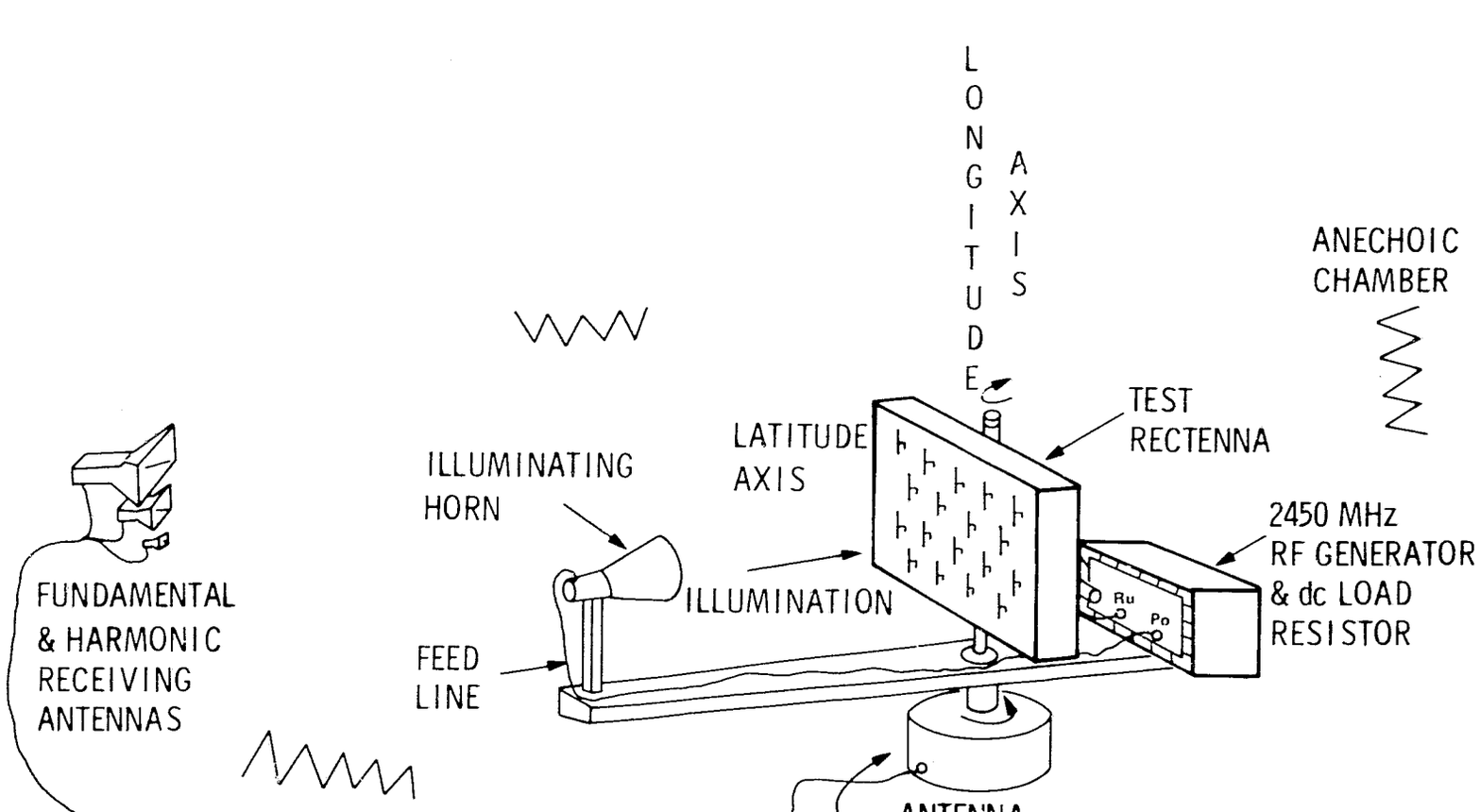

Figure A-9. Rectenna Pattern Test Setup

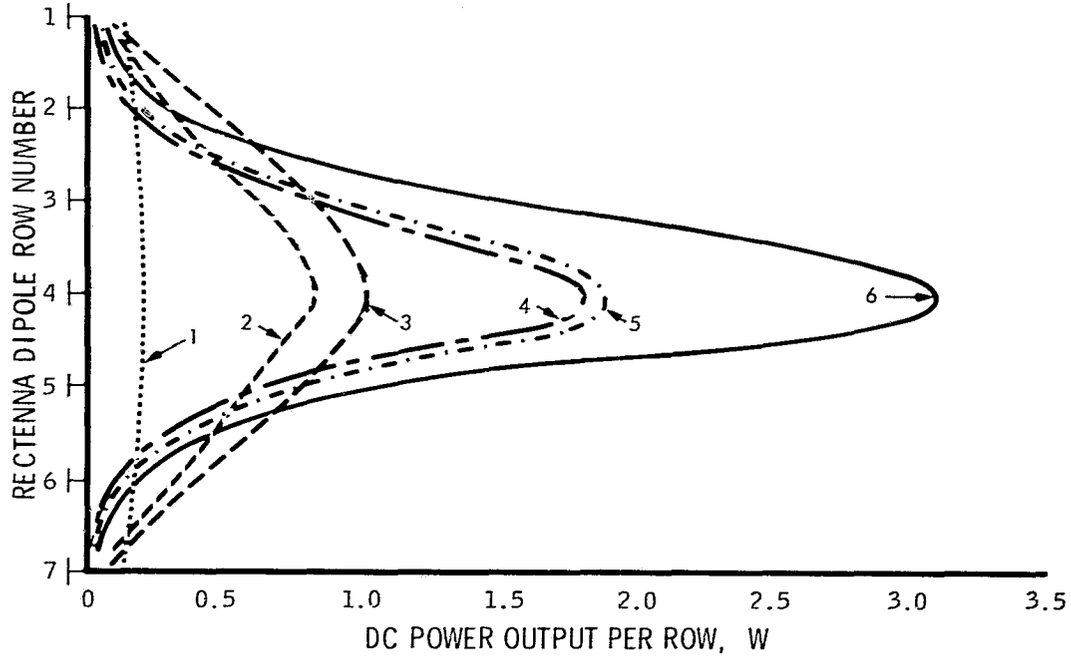

SUBARRAY OPERATING CONDITIONS & PERFORMANCE AT 2.45 GHz

CURVE	ILLUMINATOR SPACING, cm	LOAD RESISTANCE Ω	PEAK FLUX DENSITY mW/cm^2	TOTAL DC POWER OUTPUT, W	COLLECTION-CONVERSION EFFICIENCY %
1	80	15.0	2	1.29	7.4
2	40	7.5	8	2.9	16.7
3	40	15.0	8	3.63	21.0
4	20	15.0	14	3.51	27.0
5	20	7.5	32	3.97	19.8
6	20	15.0	32	6.1	35.0

Figure A-10. Rectenna Dc Output Distributions

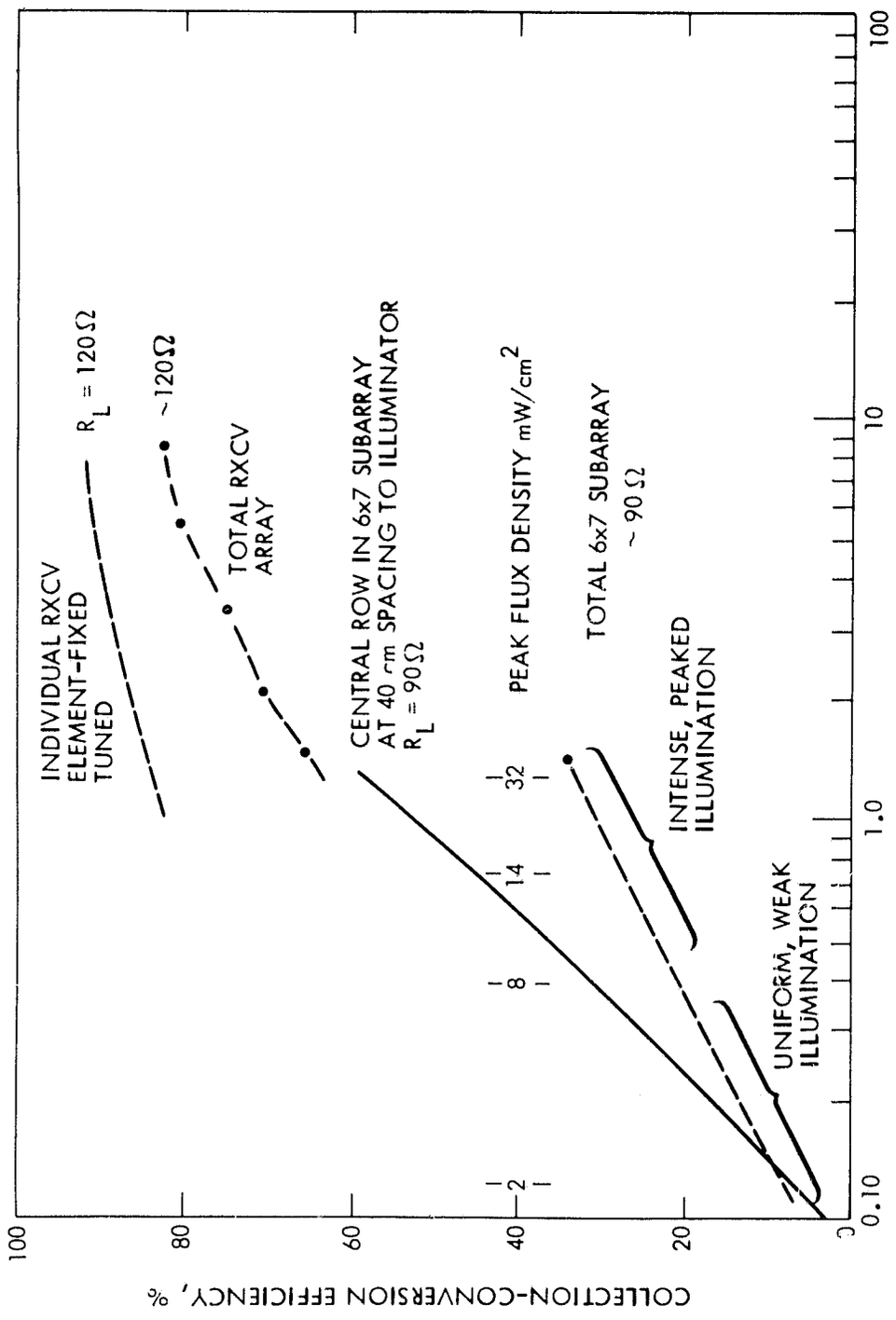

Figure A-11. Rectenna Element, Row and Array Efficiencies

angular $\cos^{1.8}\theta$ measured pattern of an operating dipole rectenna. Therefore the reflected pattern is not merely a simple reflection of the illuminator in the subarray, as significant rephasing of the illumination occurs.

Precautions were taken to assure that the harmonic patterns were verified as coming from the rectenna elements and not from the illumination TWTA RF output, by employing the tactic of running a pattern with the rectenna replaced by a flat sheet of aluminum. Additionally, there was a low-pass filter with a 2500 MHz cutoff frequency connected in the TWTA output.

The recorded pattern accuracy is estimated to be ±1 dB at the peak of the reflected fundamental, and ±2 dB per 10 dB below the peak. The harmonic accuracy was only about ±3 dB for the peak, relative to the fundamental, and ±4 to 5 dB per 10 dB below their peaks.

Different angles of incidence of the illumination up to 60 degrees were recorded. The net result was that the rescattered patterns also shifted in angle for the fundamental frequency energy.

APPENDIX B

BIBLIOGRAPHY OF RF POWER AMPLIFIER NOISE AND HARMONICS DATA

1. Special Report, "Microwave Power Sources", Microwave Journal, April 1975.

2. Data Sheet, 5K70SG 24 kw CW S-band Power Amplifier Klystron, EIMAC, A Division of Varian, San Carlos, Ca., 1965.

3. Raytheon Application Notes, "Carrier Noise Analyzer," PT-4997, 15 June 1977.

4. Sharp, E. D., and Jones, E. R. T., "A Sampling Measurement of Multimode Waveguide Power, "IRE Transactions on Microwave Theory and Techniques, Vol. MTT-10, pp. 73-82, Jan. 1962.

5. Price, V. G., "Measurement of Harmonic Power Generated by Microwave Transmitters," IRE Transactions on Microwave Theory and Techniques, Jan. 1959.

6. Nelson, R. B. et al., "Research and Experimental Study for the Development of a 1000-Watt CW Space Environment S-Band Power Amplifier," Varian Associates, NASA CR-66648.

7. Goldfinger, A., "Study Program for Re-Design of VA-949J X-Band High-Power Klystrons," Final Report, Varian Associates, Inc., JPL Contract No. 954502, Feb. 1977.

8. La Rue, A., "High Efficiency Klystron CW Amplifier for Space Applications," Varian Associates, Inc., Slide Presentation and Discussion, Feb. 1976.

NASA—JPL—Coml, L A, Calif